Pauli Valkjärvi

Integrated Data Acquisition for State-of-the-Art Large-Bore Engine Test Cell

School of Technology and Innovations
Master's thesis
Smart Energy

Vaasa 2022

VAASAN YLIOPISTO
Tekniikan ja innovaatiojohtamisen yksikkö
Tekijä: Pauli Valkjärvi
Tutkielman nimi: Integroitu tiedonkeruujärjestelmä suurisylinterisen moottorin tutkimukseen
Tutkinto: Diplomi-insinöörin tutkinto
Koulutusohjelma: Smart Energy
Työn valvoja: Apulaisprofessori Maciej Mikulski
Ohjaaja: Tohtoriopiskelija Michaela Hissa
Vuosi: 2022 **Sivuja:** 118

TIIVISTELMÄ:

Polttomoottoreilla tulee olemaan tärkeä rooli hiilidioksidipäästöjen vähentämisessä ja kestävän voimansiirtojärjestelmän toteuttamisessa merenkulkualalla. Merenkulkualan sähköistäminen on nykyisellään hankalaa valtavan energiantarpeen vuoksi. Sen vuoksi polttomoottorit tulevat pysymään lähitulevaisuudessakin laivojen tärkeimpänä voimanlähteenä. Uutta palamismenetelmää, reaktiivisuudella hallittua puristussytytystä (RCCI), voidaan pitää yhtenä lupaavista polttomoottoriteknologioista, jonka avulla voidaan samanaikaisesti saavuttaa erittäin alhaiset typen oksidi- ja hiukkaspäästöt, sekä korkea hyötysuhde. Vaikka konseptia on kehitetty pitkään, soveltuvuutta isosylinterisissä moottoreissa ei ole osoitettu julkisesti.

Tämän opinnäytetyön tavoitteena oli suunnitella ja toteuttaa uusi tiedonkeruujärjestelmä isosylinteriseen RCCI -testipenkkiin Vaasan yliopiston VEBIC moottorilaboratoriossa osana Clean Propulsion Technologies (CPT) -projektin työpakettia 3. Testipenkki instrumentoitiin uusilla antureilla, analysaattoreilla ja tiedonkeruulaitteilla. Järjestelmän rakentamiseen tarvittavat laitteet hankittiin ja laiteasennukset sekä sähköliitännät toteutettiin. Lisäksi mahdollistettiin uuteen järjestelmään soveltuva tiedon tallennusprosessi. Järjestelmän suorituskyvyn arvioimiseksi suoritettiin osittainen järjestelmätesti, koska moottoria ei ollut mahdollista käynnistää vielä opinnäytetyön aikana.

Osittaisen järjestelmätestin tulokset osoittivat, että uusi tiedonkeruujärjestelmä kykenee mittaamaan korkealla näytteenottotaajuudella ja tallentamaan mittaukset kampiakselin asennon suhteen. Opinnäytetyössä suunniteltu ja toteutettu järjestelmä tarjosi useita parannuksia edelliseen järjestelmään verrattuna. Käytettävissä olevien korkean näytteenottotaajuuden kanavien lukumäärä kasvoi 8:sta 16:een ja järjestelmä tarjoaa joustavamman reaaliaikaisen tiedon jälkikäsittelyn. Päivitetty järjestelmä tarjoaa myös merkittävän parannuksen datan integroimiseen, koska nopeat ja hitaat mittaukset voidaan tallentaa samaan tiedostoon. Välittömien järjestelmän parannusten lisäksi uusi järjestelmä kykenee mukautumaan tulevaisuuden tarpeiden mukaan.

AVAINSANAT: Tiedonkeruu, mittaaminen, anturit, RCCI, polttoanalyysi, moottoritestisolu, integrointi.

UNIVERSITY OF VAASA
School of Technology and Innovations
Author: Pauli Valkjärvi
Title of the thesis: Integrated Data Acquisition for State-of-the-Art Large-Bore Engine Test Cell
Degree: Master of Science in Technology
Degree Programme: Smart Energy
Supervisor: Associate Professor Maciej Mikulski
Instructor: Doctoral student Michaela Hissa
Year: 2022 **Pages:** 118

ABSTRACT:

Internal combustion engines will have an important role on a road to decarbonization and a sustainable powertrain system in the maritime sector. Electrification of the maritime sector is currently difficult due to its excessive energy density demand. Therefore, internal combustion engines will remain a primary power source for ships in the near future. A novel combustion concept, reactivity-controlled compression ignition (RCCI), can be seen as one of the promising combustion technologies that enables simultaneous ultra-low NOx and soot emissions, as well as high thermal efficiency. Although the concept has been developed for a long time, its feasibility for large-bore engine applications has not been publicly demonstrated.

The goal of this thesis was to design and implement a new data acquisition system for the large-bore RCCI test bench in University of Vaasa's VEBIC engine laboratory, as part of the Clean Propulsion Technologies (CPT) project's work package 3, novel combustion and advanced aftertreatment. The test bench was instrumented with new sensors, analyzers and data acquisition hardware. Devices required to build the system were acquired and device installations, as well as electrical connections were established and supervised. Additionally, data storing workflow, suitable for the new system, was developed. In order to validate the system performance, a partial system test was carried out due to the inability to start up the engine during the thesis.

The results from the partial system test proved that the new data acquisition system is able to measure high sampling frequency signals and record them in reference to crank angle. The system that was designed and implemented in the thesis provided several improvements when compared to the previous system. The number of available high sample frequency channels increased from 8 to 16 and the system provides more flexible real-time post-processing capabilities. The upgraded system also provides a significant improvement in integration, as the high-speed and low-speed measurements can be recorded into a single file. In addition to immediate system improvements, the new system is able to expand according to future requirements of the test bench.

KEYWORDS: Data acquisition, measurement, sensors, RCCI, combustion analysis, engine test cell, integration.

Foreword

This Master's thesis was done for the University of Vaasa as a part of the CPT project's work package 3. The work done in the thesis was meant as an enabler for the demonstration of a medium-speed engine utilizing low-temperature RCCI.

Firstly, I want to thank my instructor and team leader, Doctoral student Michaela Hissa for her valuable guidance throughout the thesis. I want to also thank my supervisor, Associate Professor Maciej Mikulski for supervising the work and providing useful comments and suggestions. I am also grateful for the help and support I received from the VEBIC engine laboratory staff during the implementation phase of the work.

Lastly, I am forever grateful for the support I received from my family and friends throughout my studies.

Contents

Figures

Tables

Abbreviations

ACT	Advanced combustion technology
ADC	Analog-to-digital converter
AI	Analog input
AO	Analog output
BDC	Bottom dead center
BMEP	Break mean effective pressure
CAD	Crank angle degree
CAN	Controller area network
CDC	Conventional diesel combustion
CEA	Combustion engine analysis
CLD	Chemiluminescence detector
CO	Carbon monoxide
CO_2	Carbon dioxide
COV_{IMEP}	Covariance of IMEP
CPT	Clean Propulsion Technologies
CSV	Comma-separated values
DI	Digital input
ECU	Engine control unit
EHVA	Electro-hydraulic valve actuation
EIL	Engine-in-the-loop
EOI	End of injection
FID	Flame ionization detector
FMEP	Friction mean effective pressure
FSO	Full-scale output
FTIR	Fourier transform infrared
H_2O	Water vapor
HIL	Hardware-in-the-loop
HT	High temperature

$IMEP_g$	Gross indicated mean effective pressure
$IMEP_n$	Net indicated mean effective pressure
I/O	Input/output
LT	Low temperature
LTC	Low-temperature combustion
MIL	Model-in-the-loop
NDIR	Nondispersive infrared
N_2	Nitrogen
NO_x	Nitrogen oxides
O_2	Oxygen
PLC	Programmable logic controller
PM	Particulate matter
PMD	Paramagnetic detection
PMEP	Pumping mean effective pressure
PRT	Platinum resistance thermometer
RCCI	Reactivity-controlled compression ignition
RCP	Rapid control prototyping
rpm	Revolutions per minute
RTD	Resistance temperature detector
RTU	Remote terminal unit
SiO_2	Silicon dioxide
SOI	Start of injection
SO_x	Sulfur oxides
TCP/IP	Transmission control protocol/internet protocol
TDC	Top dead center
TEDS	Transducer electronic data sheet
THC	Total hydrocarbons
TTL	Transistor-transistor logic
USB	Universal serial bus
VDC	Voltage direct current

VEBIC	Vaasa Energy Business Innovation Center
ZrO_2	Zirconium dioxide

Greek Letters

γ	Polytropic coefficient
ε	Emissivity
θ	Crank angle
ρ_v	Fluid density
σ	Stefan-Boltzmann constant
σ_s	Standard deviation

Other Symbols

A_{cyl}	Area of the cylinder wall
A_{eff}	Effective valve area
C_c	Cable capacitance
C_r	Amplifier feedback capacitor capacitance
C_t	Sensor capacitance
E	Measurement error
f	Frequency
h_c	Heat transfer coefficient
m	Mass
n	Crank angle interval resolution
N	Engine rotational speed
p	Pressure
Δp	Zero-level correction offset value
p_n	Cylinder pressure at reference point
P_b	Brake power
P_r	Pressure ratio

Q	Piezoelectric charge
Q_{gross}	Gross heat release rate
Q_{ht}	Heat loss
Q_{net}	Net heat release rate
R	Gas constant
R_{i}	Cable resistance
$R\mathrm{t}$	Amplifier resistance
t	Time
T_{g}	Temperature of in-cylinder gas
T_{in}	Temperature of intake air
T_{w}	Temperature of cylinder wall
U_{is}	Reference isentropic fluid velocity
U_{o}	Amplifier output voltage
V	Volume
V_{n}	Cylinder volume at reference point
W_{b}	Brake work
W_{i}	Indicated work
x_i	Measured variable
Δx_i	Uncertainty of measured variable
x_j	Systematic error component
Y	Calculated variable
ΔY	Uncertainty of calculated variable

1 Introduction

1.1 Background

The special report on global warming by the Intergovernmental Panel on Climate Change states that if global warming were to exceed 1.5 °C compared to the pre-industrial era, there would be significant harm to the ecosystem and societies (Masson-Delmotte et al., 2018). In 2019, the shipping industry's global carbon dioxide (CO_2) emissions accounted for roughly 2.5% of overall global CO_2 emissions (Teter et al., 2020). In addition to this, the shipping industry has a significant impact on human health and air quality near ports due to the high rate of air pollutants like nitrogen oxides (NO_x), particulate matter (PM) and sulfur oxides (SO_x) (Chen et al., 2021). Without major development steps toward more sustainable solutions, the ratio of emissions resulting from shipping compared to other transportation subsectors will increase in the future (Mestemaker et al., 2020). Paris agreement (United Nations, 2015) together with tightening emission legislation drives engine and powertrain development towards higher efficiency and lower emissions. In the heavy-duty road transport sector, the introduction of Euro VI emission standard (European Union, 2009) presented a significant NO_x emission reduction for diesel engines in order to improve the quality of air. The reduction of NO_x emissions needs to be carried out without sacrificing the inherent advantages of diesel engines or adding to other emissions. The limit of heavy-duty vehicle NO_x emissions in Euro VI compared to Euro V was reduced by 80% in steady-state testing and 77% in transient testing (Williams & Minjares, 2016). Emission legislation is one of the key drivers in the engine development process, and progress in the automotive segment inspires emission mitigation in other transport segments.

Diesel engines, commonly used in ships and heavy-duty vehicles, have a high thermal efficiency because of the high compression ratio and low heat rejection. However, they

suffer from large NO_x and PM emissions due to high in-cylinder temperatures and diffusion combustion inherent to the diesel combustion process (Wei & Geng, 2015). Advanced combustion technology (ACT) is a concept which aims to mitigate emissions while improving engine efficiency. According to Shim et al. (2020), novel combustion technologies allow for reducing NO_x and PM emissions by controlling the maximum in-cylinder temperature, as well as the local equivalence ratio. Shim et al. (2020) stated, that single-fueled ACTs offer lower emissions. However, in addition to having a narrow operating range, there are difficulties in the control of the combustion phase and maintaining combustion stability.

To overcome issues of single-fueled ACTs, researchers have investigated the possibilities of dual-fueled ACTs. According to Baškovič et al. (2022), RCCI has the highest potential among several low-temperature combustion (LTC) ACT concepts when it comes to fuel-flexibility and wide operating range. RCCI uses in-cylinder blending of two fuels with different reactivities to control combustion, which is driven by chemical kinetics (Paykani et al., 2016). In dual-fuel RCCI, low reactivity fuel is supplied into the cylinder during the intake process through a port fuel injector to create a uniform mixture of air and fuel. High reactivity fuel is injected directly into the cylinder using a single or multiple injection strategies early enough to form a premixed charge inside the cylinder prior to auto-ignition (Li et al., 2017). Changing the ratio of these two fuels, as well as the injection timing enable efficient control over the ignition timing and combustion rate (Panda & Ramesh, 2022). With RCCI, it is possible to simultaneously achieve high thermal efficiency and low NO_x and PM emissions (Krishnamoorthi et al., 2019).

Kokjohn et al. (2011) demonstrated that when compared to a conventional diesel engine, RCCI provides improved control of the combustion process, higher efficiency and significantly reduced NO_x and PM emissions in the span of a wide engine operating range. In contrast to the benefits of RCCI, there are challenges to achieve high and low engine loads. During low load operation, RCCI engines tend to have an increased rate of total

hydrocarbons (THC) and carbon monoxide (CO) due to low temperatures inside the cylinder during combustion. Additionally, operating an RCCI engine at high loads can result in excessive pressure rise rates that could damage the engine (Li et al., 2017).

Novel combustion technologies give new requirements to data acquisition system of an engine test facility. In contemporary engine research, test cells are complicated systems filled with specific machinery and instrumentation. Accurate and precise measurements need to be made in order to accurately control and capture the performance characteristics of the engine and related subsystems. A common data acquisition system comprises of an instrument that produces a signal representing the physical phenomena, signal conditioning to protect the signal from corruption and ensure signal compatibility with the rest of the system, acquisition hardware for converting analog signals to digital format, and software that is used to record, analyze and store the digital values representing the real phenomenon (Osman & Massoud, 2013). In order not to compromise the data produced in the test cell, all the devices connected to the measurement chain are desired to be integrated (Martyr & Plint, 2012). Instrumentation of modern engine test cell measurement chain includes a large variety of sensors, actuators and analyzers, each with their preparatory sensor output types and communication protocols (Asad et al., 2011).

1.2 Problem formulation

In the CPT consortium (Clean Propulsion Technologies, 2021; Mikulski, 2021), the goal is to create a shared vision and sustainable business solutions in the marine and off-road segments in order to secure the global position of the Finnish powertrain industry. The goal will be achieved by developing innovative powertrain technologies that comply with emission regulations until 2035. Technological roadmap providing a consolidated plan in securing emission compliance for both segments until 2050 will achieve the goal in the long term. The CPT project consists of six work packages. In work package 3, novel combustion and advanced aftertreatment, the goal is to provide significant progress in the

technological roadmap for novel combustion technologies. This will be made possible by demonstrating a medium-speed engine that uses low-temperature RCCI.

In order to build a large-bore RCCI marine engine platform as a part of the CPT project, many modifications are needed in the University of Vaasa's VEBIC (Vaasa Energy Business Innovation Center) engine laboratory. In this regard, the large-bore engine test cell requires new data acquisition system and measurement workflow. **The goal** of this thesis is to design and implement a data acquisition system for large-bore state-of-the-art engine test bench. New sensors, analyzers and data acquisition hardware were studied and implemented to the current engine test cell. **The objective** of this research is to discover the requirements for the new data acquisition system in order to provide more fluent low-temperature combustion research for the RCCI engine. Based on the requirements, a new measurement system was designed and implemented into University of Vaasa's large-bore engine test cell located in the VEBIC laboratory building. While realizing this objective, this work aims to answer the four following research questions:

1. What are the measurement system requirements to enable LTC research on a multi-cylinder engine?
2. How to integrate different measuring instruments into a common data acquisition platform, bearing in mind their individual sampling rates and communication protocols?
3. How to carry out efficient post-processing of the measured quantities, that enables insight to the in-cylinder phenomena?
4. How to effectively store large amount of measurement and analysis data coming from an engine test bench?

1.3 Thesis structure

This thesis consists of five main chapters which are literature review, object and methods, system design and implementation, system consolidation and validation, and conclusions. The literature review focuses on state-of-the-art engine testing and the main concepts around the engine test cell data acquisition systems. In addition, central post-processing methods and combustion analysis are discussed. The chapter provides insight regarding modern measurement technologies and analysis methodologies for conducting modern combustion engine research. Ultimately, this gives a solid background for understanding the objects and methodologies used in this work. Objects used in this research, as well as system design and validation methods are introduced and discussed in chapter 3. That chapter provides detailed information regarding the status of the test cell prior to modifications and methods to design and build a robust test cell data acquisition system. chapter 4 focuses on describing the system design and implementation phase. There, configuring and adding new measurement devices to a common system, as well as the relevant functions of the system are explained in detail. Results regarding system consolidation and validation are discussed in chapter 5. The focus is on the overall performance of the upgraded system and its adaptability for the future. The conclusions of this thesis are presented in chapter 6, which aims to give concrete answers to research questions. The final chapter of the thesis provides a summary.

2 Literature review

2.1 State-of-the-art in engine testing

Modern engine testing involves the combination of different research and development methodologies for different purposes. Simulation models coupled together with the engine test bench offer a flexible and efficient platform for engine development. This type of setup requires accurate measurement of many different parameters that are used in the calibration and optimization of the engine control system.

2.1.1 Development trends of internal combustion engines

The objective of engine development today is to produce engines with high efficiency and performance while having low emissions. Characteristics of modern diesel engines include a combustion chamber utilizing four valves, multiple common-rail injectors with high pressure of up to 2000 bar, advanced supercharging, controlled exhaust gas recirculation, oxidation catalyst, and a high level of electronic engine management (Heywood, 2018). Development trends of diesel engines aim towards improvements in common-rail direct injection, turbocharging, exhaust aftertreatment systems, and modification of the combustion process (Isermann, 2014).

Improving the combustion process and lowering emissions and noise with common-rail direct injection is possible with piezoelectric injectors that allow efficient use of different combinations of injection pulses (Wang et al., 2020). More efficient turbocharging is attained with regulated two-stage turbocharging or variable geometry turbocharging. These technologies allow high-pressure boosting, thus improving the power density and low-speed torque characteristics of the engine (Wang et al., 2020). According to Iser-

mann (2014), exhaust aftertreatment development is focusing on oxidation catalyst converters and particulate filtering in order to mitigate CO, THC, NO_x and PM tailpipe emissions. For heavy-duty engines, selective catalytic reduction appears as an alternative aftertreatment technology. With advanced combustion technologies, it is possible to significantly reduce emissions, while simultaneously having high thermal efficiency. ACTs related to diesel engine development listed by Wang et al. (2020) include homogenous charge compression ignition, dual fuel RCCI, and dual fuel highly premixed cool combustion. These combustion concepts require more sophisticated control compared to conventional diesel combustion (CDC). A good overview of these enabling control technologies can be found in the work by Duan et al. (2021), including multi-pulse injection, fast thermal management, variable valve actuation, variable compression ratio, on-board fuel reforming, and many other control functions.

2.1.2 Engine testing in general

The purpose of engine testing and research is to compare the performance of engines in different conditions and states. As outlined in the previous subsection, internal combustion engines are complex machines that require many auxiliary systems and support services in order to perform as desired. A facility designated for engine testing requires advanced control and a data acquisition system to carry out the required test procedures (Atkins, 2009). Tightening regulations, especially emission legislation has considerably shaped the scope and methods of engine testing in the individual development stages.

The first stage in engine development process is to gain an understanding of the engine performance at a fundamental level. At this level, performance is mainly influenced by the combustion event occurring inside the engine cylinder. Fundamental research is often first conducted on a single-cylinder research engine test bench. The single-cylinder engine gives a possibility of finding out performance characteristics and refining certain designs before moving to multi-cylinder configurations (Martyr & Plint, 2012). The main

advantages of a single-cylinder setup are relatively low cost and effective implementation. Optical versions of single-cylinder configurations usually have cylinder walls and piston crown made out of transparent material. This allows visual access into the combustion chamber by using a high-speed camera and enables visual observation of several in-cylinder phenomena, like combustion, flame growth and propagation, and injection-related events (Martyr & Plint, 2012). An example of an optical setup done on a medium-speed engine can be found in a publication from Merts et al. (2021). The authors conducted an optical study that enabled visualization of ignition and combustion events of conventional dual fuel and RCCI operation.

After fundamental experimentation is done with a single-cylinder setup, more applied level research is required. As stated by Asad et al. (2011), single-cylinder engine test benches often require the sub-systems to be externally established and controlled. It was also noted that intake and exhaust flows can be highly pulsating in single-cylinder configurations, which may lead to uncertainty during the measurement campaign. To properly develop and calibrate the engine control system with accurate and reliable measurements from the engine on an applied level, multi-cylinder testing is necessary. The final phase in the engine development process is to optimize the operating parameters and control functions, as well as get the certifications in a real-world test (Isermann, 2014). Figure 1 elaborates the engine research and development process discussed above and highlights the requirements for experimental setup in a specific development phase.

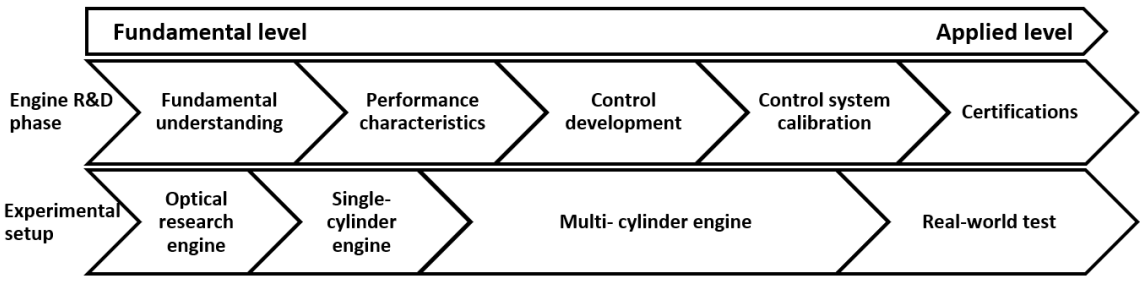

Figure 1. Overview of the engine research and development process.

2.1.3 Modern test bench and control development methodologies

According to Isermann (2014), a typical test bench consists of an internal combustion engine under investigation and a dynamometer used to convert the mechanical power generated by the engine into electrical energy. This setup is then equipped with specific instruments for control activities and required measurements. Depending on the application and desired operation profiles, different types of dynamometers are used. For example, eddy-current dynamometers are common in steady-state tests, while electric motors with grid coupling can be further applied in transient campaigns (Atkins, 2009). The main controllable parameters in the engine test bench are engine load and speed (Martyr & Plint, 2012). Aside from this, the test bench automation system regulates coolant, lubrication oil, fuels, and intake air. In addition, information is acquired from the measurement devices. Acquired information is then used in the implementation of safety and emergency procedures. Modern engine control parameters need to be calibrated to be suitable in certain operating conditions while maintaining the desired performance and emission characteristics. This procedure known as engine mapping is usually done in test benches capable of simulating real-world conditions, which helps to determine engine boundaries and optimal operating parameters in different circumstances (Martyr & Plint, 2012). However, developments in computation capacity has enabled efficient real-time calculation of combustion parameters. This in turn has led to development of engine control concepts such as closed-loop combustion control, which is crucial in RCCI to achieve stable combustion (Indrajuana et al., 2016).

Modern engine development relies on the integration of simulations and modeling together with physical testing. The early phase of engine control function and software development can be done with model-in-the-loop (MIL) simulations, where both engine and engine control unit (ECU) are simulated. This enables the design of new control functions before implementing them to an engine on a real test bench (Isermann, 2014). According to Isermann (2014), considerable time savings can be achieved with rapid control prototyping (RCP) by testing new control functions with the help of a special real-

time computer in parallel with the ECU. These new control functions operate through ECU in a bypass mode utilizing its interfaces. RCP is possible if some control functions from a previously developed ECU are usable on an engine test bench to enable testing of new functions together with the real engine and ECU. Figure 2 visualizes the principle of MIL and RCP development methods.

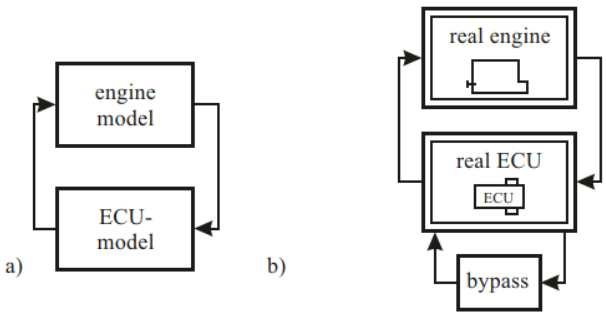

Figure 2. Principles of MIL (a) and RCP (b) methods in engine control development (Isermann, 2014).

Jiang et al. (2009) say that hardware-in-the-loop (HIL) testing is commonly used methodology for control system prototyping, calibration, and validation in modern engine testing and development. HIL enables the calibration of ECU in parallel with the mechanical development of the engine. In the HIL methodology for engine control development, real ECU is used to operate a real-time engine model. The main advantage achieved in HIL testing is that the full operating range of ECU can be tested under real-time constraints without the high cost associated with real engine tests, or possible risk of damage involved in the process of exploring the boundary conditions and abnormal operation (Martyr & Plint, 2012). According to Isermann (2014), special electronic modules are used to simulate the necessary sensor signals and outputs from the ECU can be used to operate real actuators. Figure 3 demonstrates the principle idea behind HIL testing, where a real ECU is used to operate real components together with a simulated real-time engine model.

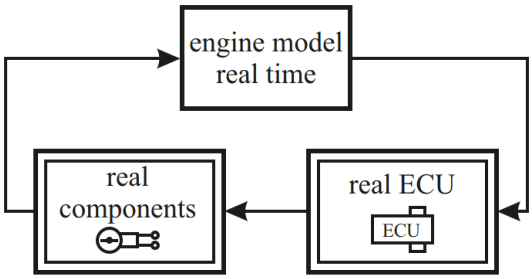

Figure 3. Principle of HIL simulation for engine control development (Isermann, 2014).

Engine-in-the-loop (EIL) simulation is a specific form of HIL simulation, as stated by Jiang et al. (2009). The real component in the EIL simulation is the engine control system together with the engine, while the simulated component is the application that the engine is coupled to. Figure 4 shows the principle of an EIL setup, where vehicle simulation is coupled to an engine test bench. Measured values from the test bench are inputs to the simulation. ECU controls the engine according to the simulation.

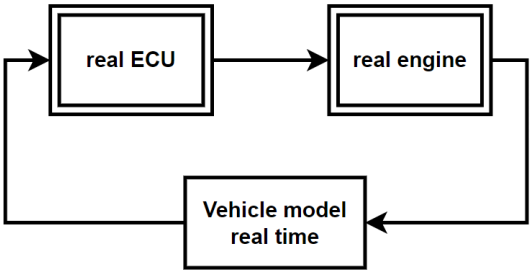

Figure 4. Principle of EIL simulation setup.

There are several advantages associated with EIL testing according to Jiang et al. (2009). It enables fast and efficient evaluation, verification, and debugging of engine control system at an early stage of development. Development of transient engine control and initial calibration focusing on the vehicle system becomes possible prior to physical vehicle integration. Simulating the vehicle allows for a fast modification of its parameters in order to learn about their impact on engine performance and behavior. Generally, the EIL test bench provides consistent and repeatable test runs (Jiang et al., 2009). Klein et al. (2017) discuss the quality of EIL testing and say that it is dependent on the simulation models, parameter accuracy, and implementation with the test bench. They also point

out that despite the benefits of EIL, model integration with the test bench may require too many resources to justify the effort.

2.2 Test bench transducer and analyzer technologies

Accuracy of the measurements in modern engine research and testing is important. Even though the measurement chain depends on the experimental setup, a large number of different parameters exhibiting dependency on each other need to be measured from internal combustion engines (Asad et al., 2011). There is a substantial number of different transducers and analyzers needed in order to enable required measurements during modern engine testing.

2.2.1 Angular position and speed measurement

According to Rogers (2010), basic engine speed and phase measurements can be done using the inductive measurement principle where an inductive position sensor consisting of a permanent magnet and coil is mounted near the engine flywheel in a way it detects the change in magnetic flux due to passing gear teeth. Flux density is at its peak when the air gap between the tooth and the sensor is at its smallest, indicating that a tooth is positioned perpendicular to the sensor. This changing magnetic flux induces an alternating sine current in the coil that represent the engine speed and phase (Rogers, 2010). A digital Hall effect sensor can also be used similarly to generate a signal for the indication system (Merker et al., 2012). Gear tooth-based sensors are often used only in monitoring and speed measurement applications due to relatively low angle resolution for combustion measurements (Rogers, 2010).

The use of a crank angle encoder is crucial for combustion measurement as it is used to provide a reference crank angle for the measurement system (Rogers, 2010). An angular

encoder is mounted to the end of the crankshaft and consists of a disk that spins together with the crankshaft. Because the position of the encoder is used to indicate the position of the crankshaft, it is crucial to properly install the encoder (Martyr and Plint, 2012). The disk has light gates engraved in it and the encoder produces a pulse each time that light passes through a gate. Spinning movement of the disk results in a square wave signal. When the exact number of pulses that the encoder produces during one revolution is known, pulse count and the frequency of the wave signal will determine the angular position and the speed of the crankshaft (Rogers, 2010). There is usually one additional output signal that is used as a trigger signal for determining when the crankshaft has rotated a full revolution. This trigger pulse is generated with an additional light gate in the disk. Figure 5 below illustrates the working principle of the gear tooth sensor and optical encoder.

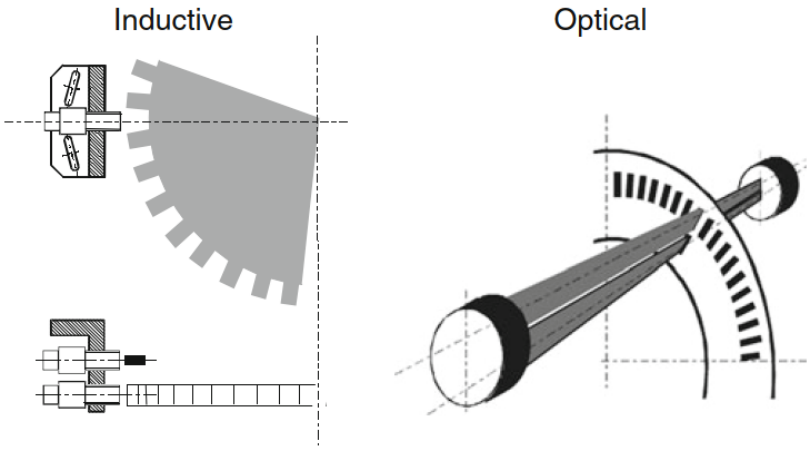

Figure 5. Measurement principles of gear tooth sensor and optical encoder (Merker et al., 2012).

2.2.2 Linear displacement measurement

Movement in one direction is called linear displacement. Displacement and position are measurements often needed in engine testing for determining the status and movement of actuators and valves (Martyr & Plint, 2012). The sensor that measures linear position or displacement has an output signal that represents the movement of the measured object related to the reference point. In engine research and development, there is often

a need for dynamic displacement measurements, such as injector needle lift and valve movement (Rogers, 2010). According to Martyr and Plint (2012), inductive transducers can be used in this type of measurement. The working principle of an inductive displacement transducer is based on changes in impedance between the coils of the sensor and a conductive object whose movement is being measured (National Instruments, 2021). Transducers that are based on the Hall effect are also used (Martyr and Plint, 2012). In a Hall effect transducer, a movement of a magnetic object causes a change in magnetic flux sensed by a Hall effect sensing element, which outputs a voltage signal proportional to the movement of the object (Rogers, 2010).

2.2.3 Pressure measurement

As stated by Smith (2009), pressure can be determined as a force resulting from molecules of a fluid or gas hitting on a surface of a container. Pressure can be measured in several ways. Absolute pressure measurement means that the pressure is measured relative to zero. Gauge pressure means that ambient air pressure is used as a zero reference. Differential pressure measurement is used as a difference between two points. There are typically two elements present in an electronic pressure transducer. One is the element that is used to sense the pressure, such as a diaphragm that converts the pressure into displacement. Another element is for converting the displacement into measurable electrical property.

Measuring the pressure of different mediums gives insight into the operation of the engine. According to Martyr and Plint (2012), typical mediums in an engine test cell from which absolute pressure is measured include fuel, lubrication oil, coolant, intake air, and exhaust gas. Common transducer types used for absolute pressure measurements from the engine are strain gauge and a capacitive transducer. A strain gauge transducer consists of a diaphragm that deforms according to the applied pressure. Another component of a strain gauge transducer is a strain gauge made from conductive material whose electrical resistance varies according to the change in diaphragm geometry. Transducers that

have their strain gauge made out of semiconductor material are called piezoresistive transducers (Morris & Langari, 2012). Pressure value can be derived directly from the resistance of the strain gauge, typically by using a Wheatstone bridge circuit. The sensitivity of a strain gauge transducer depends on the material of the strain gauge and is quantified by the gauge factor that describes the change in resistance relative to applied strain (Rogers, 2010). Piezoresistive transducers have significantly higher gauge factors compared to conventional metal strain gauge transducers (Morris & Langari, 2012). A capacitive pressure transducer includes a capacitor as its diaphragm and is designed in a way that allows for the capacitor's capacitance to vary according to the applied pressure (Smith, 2009).

In modern combustion engine research and development, pressure transducers that are based on the piezoelectric effect are a choice of instrumentation for in-cylinder pressure measurements because they can produce in-cylinder pressure curves with great accuracy and repeatability (Rogers, 2010). The piezoelectric effect refers to an electric charge that accumulates in certain materials, such as quartz (SiO_2), when it is placed under stress. Piezoelectric pressure transducers have a piezoelectric crystal as an element that converts the displacement into an electrical signal. The magnitude of the produced charge depends on the change in pressure and requires an amplifier circuitry to produce a strong enough signal for the acquisition system (Kistler, 2020). Figure 6 visualizes the principle of piezoelectricity, where the load applied to a quartz crystal produces a directly proportional electrical charge into the measurement circuit.

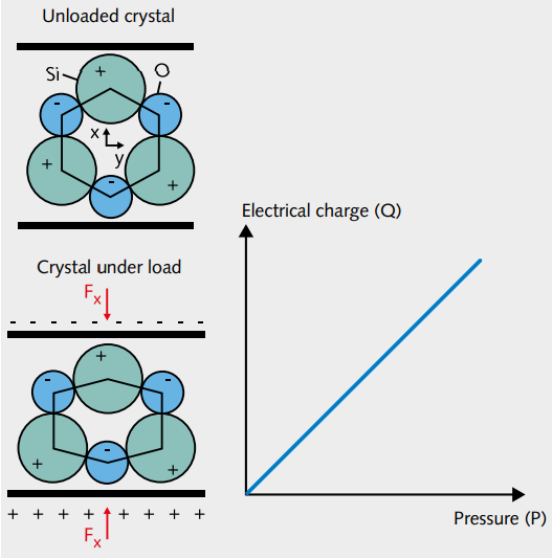

Figure 6. Piezoelectric principle (Kistler, 2020).

Piezoelectric crystal inside the pressure sensing element responds only to dynamic changes in pressure and are not suitable for absolute pressure measurements. Piezoelectric pressure transducers are relatively small in size, have a high natural frequency and large measuring range (Kistler, 2020).

2.2.4 Temperature measurement

Temperature is a parameter that provides essential information about the condition of the engine. According to Smith (2009), temperature means the ability of an object to transfer heat. The temperature sensing element needs to be in thermal equilibrium with the object or substance and therefore, the fastest response is gained when the measurement devices are in direct contact with the object of measurement. Sometimes the temperature sensing element is installed inside a thermowell. Thermowell is used to protect the sensing element from forces and chemical effects induced by the medium. A disadvantage of using a thermowell is slower response time and reduced accuracy of temperature measurement (Smith, 2009). Almost every temperature that needs to be measured during engine testing typically remains in a steady state or do not change very

much during short periods of time (Martyr & Plint, 2012). However, temperatures, especially exhaust gas temperatures, are almost never exactly stable and may vary greatly between different operating points. Averaging multiple measurements can reduce the problem of unstable gas flow resulting from pulsations coming from different cylinders. When moving from one operating point to another, it is needed to wait for the measured temperatures to stabilize in order to get reliable measurements when changing from one operating point to another. This reduces the error resulting from heat absorbed into engine surfaces and possible sensor shielding (Martyr & Plint, 2012).

Thermocouples are well suited for most temperature measurements inside an engine test cell. Thermocouples of every type consist of two wires made out of different metals that form a closed circuit consisting of two junctions, one is for reference and the other in thermal equilibrium with the object. When a temperature difference occurs between the two junctions, a current begins to flow in the closed circuit according to the Seebeck effect (Smith, 2009). The temperature value is obtained by introducing a resistor with a large resistance into the circuit and reading the voltage that is produced. This voltage across the resistor is proportional to the temperature difference between the two junctions. In theory, the Seebeck effect occurs between any two dissimilar types of metal, but due to practical reasons, current flow in relation to the temperature difference must be repeatable, high enough and as linear as possible (Smith, 2009). This means that only few different metal pairs can be used in practice. The most common thermocouple types used in engine testing facilities are types T (copper-constantan), J (iron-constantan) and K (chromel-alumel) (Martyr & Plint, 2012). As stated by Smith (2009), main advantages of thermocouples are that they can be used at high temperatures up to 1700 °C, they can withstand vibration and shock, and they are cost-effective compared to other available temperature measurement devices. Disadvantages compared to resistance temperature detectors (RTDs) are low signal level, required compensation of a reference junction, lower accuracy, and deterioration over time resulting to drift.

When temperature measurement requires accuracy and reliability beyond the capabilities of thermocouples, platinum resistance thermometers (PRTs) can be used (Martyr & Plint, 2012). PRTs are resistance temperature detectors that use platinum as a resistor element. It is known that the resistance of metals increases with temperature. The principle of PRTs is the relationship between the temperature and the resistance of the resistor. This relationship is not exactly linear and usually the nonlinearity is greater at higher temperatures (Smith, 2009). Resistance is measured by running a small current through the resistor and measuring the voltage drop. Temperature can be derived from the relationship between the resistance and the temperature. The most used type of PRT is called 100-Ω platinum RTD, which has a resistance of exactly 100 Ω at 0 °C. Because the wiring between the resistor element and the resistance reading device can introduce major error to the measurement, often 3- or 4-wire systems are used to compensate resistance of the wires. According to Smith (2009), the use of platinum as the resistor element is justified by several arguments. PRTs have a high sensitivity, meaning that the resistance of platinum changes according to temperature relatively large amount compared to other metals. Platinum also has a good resistance against corrosion. PRTs have a relatively large temperature range even up to 850 °C and linearity between temperature and resistance is decent across the whole usable temperature range (Martyr & Plint, 2012). PRTs have several advantages compared to thermocouples, such as better accuracy, stability over time and the ability to handle possible electrical interference within a test facility. Engine temperature measurements are usually required to be measured from fluid and gas flow systems and from different mechanical components (Martyr & Plint, 2012). These include intake, exhaust, coolant, oil and fuel systems, as well as related mechanical parts. In reality, the locations of the measurements may vary depending on the engine application and the purpose of testing.

2.2.5 Smart sensors

Sensors that have smart features embedded in them are called smart sensors. The Institute of Electrical and Electronics Engineers proposed an international standard called

Transducer Electronic Data Sheet (TEDS) to standardize communication between any TEDS sensor and smart signal conditioning device regardless of the manufacturers. According to Rogers (2010), the usage of TEDS depends heavily on the application area. Data contained in TEDS typically includes basic information, such as data about the sensor itself and information regarding calibration. TEDS is stored on a microchip that is usually embedded in the sensor itself or the connector and accessing the information requires the use of a specific connection. In addition to a typical connection carrying an analog signal from the transducer, a parallel connection that provides the signal conditioning system with a connection interface to the microchip is required (Rogers, 2010).

A useful feature that usually comes with smart sensors and conditioning systems is the ability to automatically record the operating data of a sensor. This means that the operating hours and cycles can be recorded in order to keep track of the planned regular checking and recalibration of the instruments (Rogers, 2010). An additional feature that has significant value in engine testing is the ability of amplifier circuitry to recognize the sensor. When it is possible to assign a sensor to a specific application, risks involving incorrect parametrization and connection of a wrong sensor are eliminated (Rogers, 2010).

2.2.6 Fuel consumption and flow measurements

Fuel consumption is an important parameter to be measured during engine testing. Accurate measurement of fuel consumption enables research and development of efficient engines with reduced emissions. According to Martyr and Plint (2012), modern engine testing requires the actual and transient measurement of fuel consumption during different test sequences. Modern engines usually incorporate fuel return strategies or fuel spillback to provide more accuracy, but in turn, increases the complexity of the engine test cell fuel consumption measurement system. In modern fuel measurement systems, it is not accurate to measure only the fuel that is being supplied to the engine. The sys-

tem needs to be able to measure the amount of fuel that enters the metering and conditioning system. This means that in order to mitigate possible sources of measurement error, the system must be able to control the pressure in the return fuel lines and remove possible vapor bubbles and heat energy that have formed while passing through the engine fuel system (Martyr & Plint, 2012).

According to Martyr and Plint (2012), the two most usual types of fuel gauges used for liquid fuel measurement are volumetric and gravimetric gauges. A volumetric gauge measures the volume of the fuel that is consumed in a specific period. Volume can be measured from a container that has a known volume or from the flow through a flowmeter. Gravimetric gauges measure the mass of consumed fuel during a specific period. As illustrated in Figure 7 below, gravimetric fuel gauges consist of a container that is mounted on a load cell that measures the weight of the container. Fuel is supplied to the engine through this container and the mass of the supplied fuel can be measured against time. Return fuel from the engine injection system is also returned to this container through spillback.

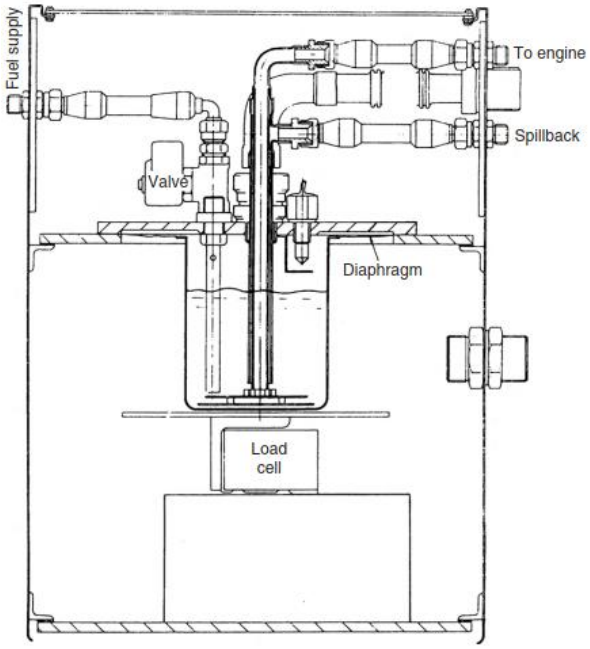

Figure 7. Structure of direct weighing gravimetric fuel gauge (Martyr & Plint, 2012).

The mass flow rate of the supplied fuel to the engine can be measured with mass flow meters. According to Martyr and Plint (2012), mass flow meters in the market are typically Coriolis flow meters that utilize the Coriolis effect. Figure 8 shows the structure of the Coriolis effect mass flow meter.

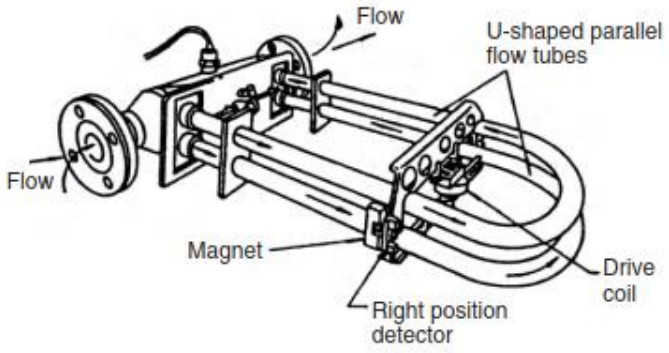

Figure 8. Coriolis mass flow meter (Martyr & Plint, 2012).

From Figure 8 can be seen that a Coriolis meter consists of two parallel U-tubes that the fuel passes through. Electromagnets are used to make the tubes vibrate at a specific frequency. When there is mass flow present inside the tubes, Coriolis force will produce an additional vibration to the tubes that results in slight differences in the relative vibration of the tubes. These differences are detected with sensors that measure the position, velocity, or acceleration of the U-tubes and produce a sinusoidal voltage signal representing the mass flow of the fuel (Martyr & Plint, 2012). The advantage of the Coriolis effect mass flow meter is its ability to continuously and accurately measure many different kinds of liquid and gaseous substances.

Air flow in the test cell can be measured with several kinds of methods such as venturi gas meter. The operating principle of a venturi meter is based on the pressure drop across a venturi inside the pipe that the air is flowing through (Martyr & Plint, 2012). According to Atkins (2009), a preferred method to measure airflow inside the engine test cell is to use square-edged orifice plates. The working principle of this method is based on the pressure drop resulting from an orifice inside the pipe. As the air flows thorough

an orifice, it causes a slight pressure difference between the different sides of the orifice. Actual air flow can be derived from the measured pressure drop across the orifice.

2.2.7 Exhaust gas emission measurement and analysis

According to Martyr & Plint (2012), there exists emission legislation for every type of machinery that uses internal combustion engines. This means that every engine needs to go through a defined test sequences in order to get the analysis of the engine exhaust composition and emissions according to procedures. The emission composition depends heavily on engine design, operating conditions and the properties and composition of the fuel used (Martyr & Plint, 2012). Gaseous components of complete combustion are nitrogen (N_2), water vapor (H_2O), oxygen (O_2), and CO_2. During incomplete combustion many other components are formed inside the cylinder and are regarded as emissions. Typical emissions are particulate matter (PM), carbon monoxide (CO), total hydrocarbons (THC), and nitrogen oxides (NO_x). Additionally, the use of diesel fuel results in SO_x emissions (Martyr & Plint, 2012). In order to measure every different component from the exhaust stream, the engine test cell needs to be equipped with measurement and analysis equipment for both, gaseous compounds and particle emissions. Instruments best suited for specific test procedures depend on individual requirements. As stated by Martyr and Plint (2012), analyzers used to measure steady-state operation are required to exhibit accuracy, sensitivity, and stability which often leads to slow response times. When emissions are measured during transient conditions, analyzers with much faster response times of a few milliseconds are required. The main factors affecting the response time are the distance between the sampling point and the analyzer, as well as the time taken to analyze the sample.

Atkins (2009) lists many elements that need to be considered in the exhaust emission sampling system regardless of the technologies used. Heated lines are required to keep the temperature of the sample gas high enough to prevent water vapor and hydrocar-

bons from condensing to the walls of the sample line. Because many analyzers are sensitive to variations in pressure and flow rate, they need to be kept constant with regulators and sample pump. Water vapor and solid particles in the sample may cause errors in some analyzers, usually those based on the absorption of infrared radiation. In the case of possible errors, they need to be filtered from the sample. The sampling system needs to be sealed properly and flushed regularly in order to prevent errors caused by leakages of air into the sampling system and contamination from previous samples.

Fourier Transform Infrared (FTIR) analyzer can be used to measure multiple gas compounds simultaneously from the exhaust stream of an engine (Heywood, 2018). The working principle of the FTIR analyzer is based on the unique spectrum produced by different atoms and molecules when they are exposed to infrared radiation. FTIR gas analyzers expose the sample gas to infrared radiation. Based on Fourier analysis of the gathered spectrum, different compounds in the gas can be identified and their amounts determined (Martyr & Plint, 2012). Almost every gaseous compound from the sample gas can be identified using an FTIR analyzer, except diatomic elements and noble gases. They are transparent in the spectrum due to them not absorbing any infrared radiation. These gases are in return used to record the background spectrum in order to eliminate it from the real test results (Gasmet, 2020). Nondispersive Infrared (NDIR) analyzer is also based on the unique infrared absorbance band of different compounds (Heywood, 2018). However, the NDIR analyzer cannot measure multiple compounds as it does not perform Fourier analysis on the complete absorption spectrum of the sample gas. Specific filters selected according to the absorbance band of the measured compounds are required. Typically, CO_2 and CO are measured using an NDIR analyzer (Martyr & Plint, 2012).

A chemiluminescence detector (CLD) is based on a phenomenon in which light is produced by certain chemical reactions. With this method, the amount of NO_x can be measured from the exhaust gas by using ozone to react with NO in the sample gas (Heywood, 2018). Following reactions produce light which is detected by a photomultiplier and the

resulting intensity is proportional to the concentration of NO_x in the sample gas (Nakamura & Adachi, 2013). The structure and operating principle of the CLD analyzer are illustrated in Figure 9.

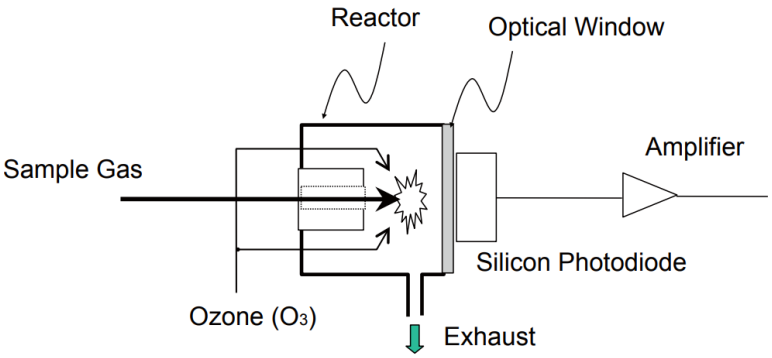

Figure 9. Structure of chemiluminescence detector measuring NO concentration (Nakamura & Adachi, 2013).

A flame ionization detector (FID) can be used to measure carbon-containing compounds from the sample gas (Heywood, 2018). It is used to measure THC concentration in exhaust gas and has a wide dynamic range and sensitivity (Martyr and Plint, 2012). The basic structure and operation principle of the FID instrument is shown in Figure 10.

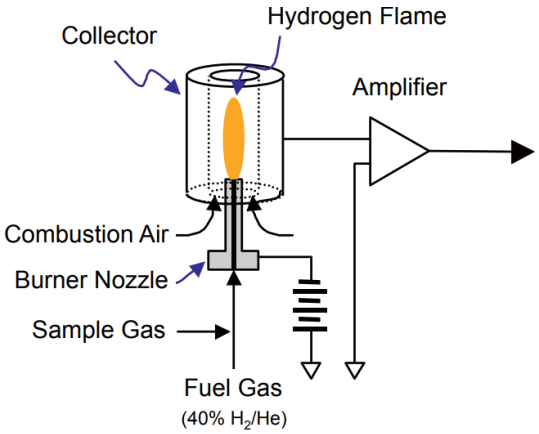

Figure 10. Structure of flame ionization detector measuring THC concentration (Nakamura & Adachi, 2013).

Inside FID, the sample gas is burned in a hydrogen flame. Burning hydrocarbons produce free electrons and positive ions that are collected with a collector electrode. When this

collector containing ions is introduced to an electric field, current will start to flow through the collector. The magnitude of the current is proportional to the ionization of the hydrocarbons and can be used to determine the concentration of hydrocarbons in the sample gas (Nakamura & Adachi, 2013). An important part of making successful emission measurements is selecting the proper measuring range with respect to expected concentrations and calibrating the analyzers according to this range (Nakamura & Adachi, 2013).

Oxygen concentration can be measured by using paramagnetic detection (PMD) analyzer (Heywood, 2018). PMD analyzer relies on strong paramagnetic susceptibility of oxygen. PMD analyzer contains a measuring cell that has a strong magnetic field inside to which the oxygen molecules will be drawn. This movement of oxygen molecules will displace a balanced detector instrument inside the measuring cell and this displacement can be measured. Displacement of the detector is proportional to the oxygen concentration in the sample gas (Martyr and Plint, 2012). Zirconium dioxide (ZrO_2) oxygen sensors are also used to compute oxygen concentration from the sample gas. It is based on the property of zirconium dioxide, where voltage is generated across the ZrO_2 element when different oxygen concentrations occur on both sides of the element (SST Sensing Ltd, 2017). The ZrO_2-based lambda sensors, such as the wide band universal exhaust gas oxygen sensor, are used in determining the air-fuel ratio to be used in engine performance and emission control. Modern and robust lambda sensors enable lambda control, which is important for combustion control in LTC concepts, such as RCCI (Kasprzyk et al., 2020). The advantage of deriving air-fuel ratio based on the output from ZrO_2 sensor when compared to multicomponent gas analyzer is that the calculation is based on a single output. This eliminates the need to consider the response times of different gas components. Additionally, on-board lambda sensors enable easier installment and good response time (Nakamura & Adachi, 2013).

Particles present in the exhaust gas are indicated by the color of the exhaust gas. As stated by Martyr and Plint (2012), opacity meters are widely used to measure the opacity

of exhaust gas. The opacity meter operates by forming a light beam across undiluted exhaust gas to the detector. The amount of light reaching the detector depends on the number and size of the smoke particles, as well as the distance between the light source and the detector. Light absorption characteristics of the smoke particles also contribute to the results. The output of an opacity meter usually represents the percentage of the light being absorbed by the exhaust gas (Martyr & Plint, 2012). The PM measuring principle can also be based on the amount of light absorbed by soot particles caught in the filter paper. Smoke meters consist of a light source, filter paper, and a light detector. The amount of light that reaches the detector through the filter paper is dependent on the amount of smoke that is filtered from the sample gas (Atkins, 2009). There are also particulate samplers that can measure the mass of the particles caught in the filter paper and optical particulate counters (Martyr & Plint, 2012).

2.3 Signal conditioning and acquisition

Signal conditioning is an essential part of a measurement chain and it is located between the sensor sending an electrical signal and a device that samples and records the signals. Signal conditioning has a huge part in overall system accuracy and different sensors each having their specific output may have different requirements for conditioning. In addition to analog signal transmission, some instruments require a digital interface in order to send the data forward. In an engine test cell, different digital transmission technologies specific to the instruments usually have to be incorporated into a data acquisition system. Figure 11 below shows the typical process of data acquisition.

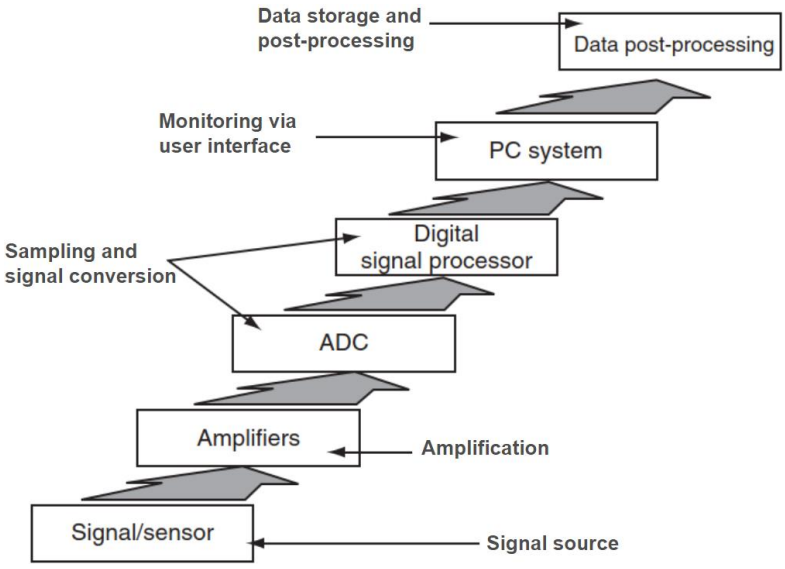

Figure 11. Principle of data acquisition process (adapted from Martyr & Plint, 2012).

Signals produced by a sensor or a transducer often require proper amplification (Morris & Langari, 2012). After signal processing, signals are sampled and digitized. After converting the analog signal to digital samples, data is transmitted for monitoring, processing, and storing.

2.3.1 Signal amplification

An electronic amplifier is a commonly used instrument in the measurement chain because a signal coming straight from the sensor often requires some form of amplification before the acquisition. This is due to the amplitude of a sensor output being too low for being measured accurately and low-level signals are more prone to electrical interference coming from outside the measurement chain. Amplifiers, therefore, improve the sensitivity and resolution of the signal (Morris & Langari, 2012). It is important to avoid any noise affecting the signal before amplification to prevent the noise from being amplified in the process. Amplifiers are best to be located as near to the sensors as possible

in order to reduce the length that the low-level signal has to travel and possibly get corrupted by electromagnetic interference (Martyr & Plint, 2012). Specific requirements and characteristics of an amplifier depend on the type of signal they are used to amplify.

According to Rogers (2010), the combustion measurement chain requires charge amplifiers that convert the charge coming from the piezoelectric pressure transducer into voltage that can be read by the measurement system. Due to the importance of in-cylinder pressure measurements in engine research, charge amplifiers are almost always present in the test cell measurement system. Figure 12 shows the main components present in the charge amplifier circuit designed for piezoelectric pressure transducers.

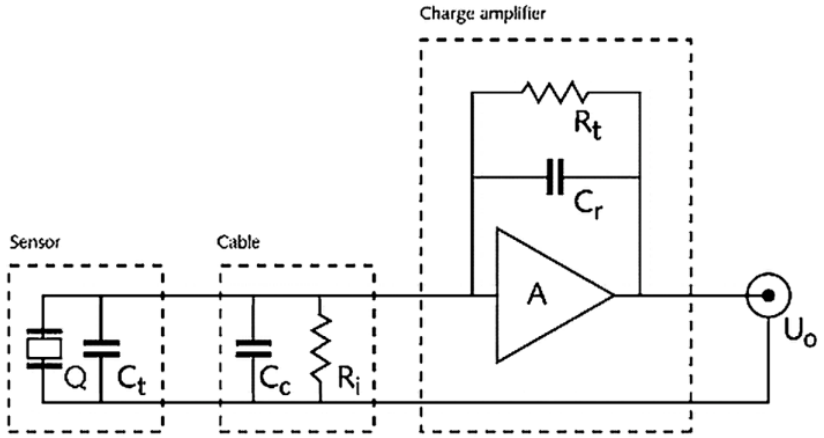

Figure 12. Basic charge amplifier circuit for a piezoelectric pressure transducer (Rogers, 2010).

As illustrated in Figure 12, a piezoelectric crystal produces an electric charge, Q, that results in a slight increase in voltage at the amplifier input which is then amplified significantly. Because the gain of the amplifier is large, capacitances resulting from the sensor (C_t) and cable (C_c) do not have a significant effect on the amplified output voltage (U_o). This leaves the output voltage to be dependent only on the magnitude of the input charge and the capacitance of the feedback capacitor (C_r) required to restrict the voltage rise at the amplifier input and reduce unwanted noise (Rogers, 2010).

2.3.2 Measurement error reduction

Measurement errors always exist to some extent in the measurement system. With a good design of the system together with proper data post-possessing and analysis methods, the impact of these errors can be mitigated. Morris and Langari (2012) divide measurement errors into two categories, errors resulting from the measurement process and errors occurring during signal transmission and conditioning.

Errors that occur during the measurement process are either systematic or random. Systematic errors consistently fall on either side of the correct reading. One source of systematic error is the changes in the physical properties of the measured process that are a result from the measurement situation. The significance of the error depends on the instruments and the measured process. In order to mitigate the error, the type of instruments must be chosen for the specific measurements. The environment will also have an effect on the measurement system by introducing an environmental input to the measurement system. These inputs are changes in the environmental conditions that have an effect on the process being measured. The effect of environmental inputs can be considered by correcting them in the output reading of the instrument or increasing the environmental resistance of the instruments (Morris & Langari, 2012). Errors induced by the environment are especially relevant in engine test conditions. Drastic temperature changes expose the transducers to the effect of drift. Also, improper mounting of the transducers together with the engine vibrating can lead to additional noise in the transducer output (Rogers, 2010). Systematic errors also arise as a result of instruments wearing down and additional resistance of the wiring used to connect the sensors to the acquisition system. The wear of the measurement instruments can often be solved by calibrating the instruments regularly. Errors due to wire resistance are mitigated by using cables with properly large cross section and planning the cable routes to be as short as possible (Morris & Langari, 2012).

Random errors are experienced as a disturbance in measured value and are a result of unpredictable variations in the measurement system. These variations can be a result of false human observations, noise caused by electrical disturbance or sudden changes in the measurement environment. According to Morris and Langari (2012), random errors in static measurements can be reduced by calculating the average result of multiple measurement points.

Errors that occur during signal transmission and conditioning mainly arise because of electrical interference resulting from nearby power cables, ground loops, poor wiring practices, analogue-to-digital conversion or other electronic devices. This interference is seen as noise in the signal and the resulting error is more significant in situations where the range of the measured signal is relatively low. This will result in a poor signal-to-noise ratio (Rogers, 2010). Current signals are inherently more resistant to noise compared to voltage signals, therefore they are preferred for long distances in noisy environments (Osman & Massoud, 2013). To prevent noise from entering the measurement system, properly shielded cables should be used for transmitting the signals and these cables should be placed as far as possible from any source of possible interference (Measurement Computing, 2012). The appearance of high-frequency noise in the signal is a common problem in most data acquisition systems and analog filtering is an effective method of getting rid of unwanted frequencies. Basic types of filters are the low-pass filter that blocks high-frequency components, a high-pass filter that blocks low-frequency components, a band-pass filter that passes only a certain frequency band, and a band-reject filter that blocks a certain frequency band. Filters can be passive or active, the difference being that active filters consist of active components, such as transistors and operational amplifiers, in addition to passive components, like resistors and capacitors. The operation of active filters is superior to passive filters, because they do not introduce as much resistance to the signal conditioning circuit as passive filters (Morris & Langari, 2012).

2.3.3 Analog-to-digital conversion

An important part of any data acquisition system is an analog-to-digital converter (ADC). The purpose of an analog-to-digital conversion is to turn analog sensor output into a binary number representing the analog measurement value. This binary number is then transformed into a base 10 digital number in the computer and displayed on a monitor (Measurement Computing, 2012). Resolution and accuracy are two main characteristics involving ADCs. The resolution of ADC is given as a number of bits that corresponds to the number of discrete steps that the digital value is able to divide the analog signal into. An n-bit resolution means that the ADC divides the measurement range into 2^n discrete steps (Measurement Computing, 2012). Therefore, the resolution of the digital value depends on the resolution of the ADC and the measurement range (Smith, 2009). Martyr and Plint (2012) note that the required resolution of ADC should be selected according to the accuracy and significance of the signal. If the inaccuracy of the signal is an order of magnitude greater than the value of a discrete step in the digital output of the ADC, it is not cost-effective and may even give a wrong picture about the accuracy of the signal. According to Asad et al. (2011), ADCs with 16-bit resolution are common in high-frequency data acquisition systems that are used in engine testing.

In measurement applications, the accuracy of the AD conversion is a critical factor. There are many possible errors during the AD conversion that can happen, some of which are practically unavoidable (Measurement Computing, 2012). In Figure 13 below, the most common types of ADC errors are presented.

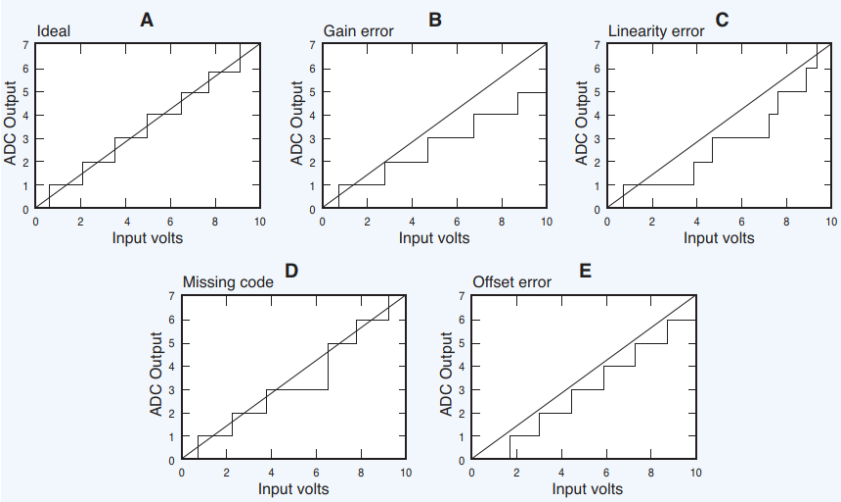

Figure 13. Most common types of errors resulting from ADCs (Measurement Computing, 2012).

In Figure 13, the straight line in each graph represent the analog output that is given to ADC and the step function represents the digital output to the acquisition system. Graph A represents the linear, therefore ideal relationship between the analog and digital outputs. Even in a situation where the relationship would be ideal, there will be restrictions in accuracy caused by the resolution. Regardless of the ADCs resolution, there will always exist small gaps between the discrete steps that the real value will most likely be in reality (Measurement Computing, 2012). Gain and offset errors, represented in graphs B and E respectfully, can be eliminated with proper calibration of the ADC and related acquisition software. Linearity error presented in graph C means that the digital output deviates from the actual analog input nonlinearly. Graph D represents a missing code error where ADC is unable to produce a digital output for a certain analog value. Linearity error and missing codes are not possible to eliminate with calibration (Measurement Computing, 2012).

2.3.4 Test cell data communication technologies

Modern engine test cells have several different equipment to be controlled and receive data from. At the same time as the need for more control has increased, also the need

for high-speed data transmission has increased. Engine test cell data transmission system has to be able to handle a two-way flow of data with high transfer rates (Martyr & Plint, 2012). Additionally, many devices used in test cell measurement and control systems have their specific requirements for data transfer protocols and standards that must be satisfied.

Controller area network (CAN) is a commonly used standard automotive engineering serial bus used to transmit data packets to every device that is connected to the network. Electronic devices connected to the network are usually sensors and actuators. According to Martyr and Plint (2012), the CAN bus is able to operate in a high-noise environment enabled by twisted pair physical media carrying a 5 V differential signal. Resistance to noise is a useful characteristic in engine test cell environment due to many possible sources of high-frequency noise.

Serial communication provides a communication link between a transmitter and a digital system. These two systems must be equipped with serial communications cards that provide a communication point for the device. According to Smith (2009), common types of protocols used in serial communications are RS-232 and RS-485. They are hardware standards, meaning that they determine for example the topology of wires in the cable and voltage levels. RS-232 is more commonly used and has a maximum distance of around 15 meters. A significant drawback of RS-232 is that it requires a common ground for a transmitter and a receiver due to a lack of electrical insulation. RS-485 is better for industrial applications because it enables longer communication distances and provides electrical isolation (Smith, 2009).

Another typical industrial connection standard found in most engine testing facilities is Universal Serial Bus (USB). It determines specifications for cables, connectors and connection protocols. Characteristics of USB are high data transfer rate and a wide range of applications with a maximum cable length of approximately 5 meters. USB has been re-

vised many times to gain faster data transfer, but all new revisions are backwards compatible with older revisions (Compaq et al., 2000). According to Morris and Langari (2012), most computer-based data acquisition systems are connected via USB connection.

Modbus is a commonly used messaging protocol for industrial applications. It was developed to exchange information between programmable logic controllers (PLCs) and a host computer (Smith, 2009). Modbus provides a client-server communication over transmission control protocol/internet protocol (TCP/IP) network between devices that are able to read and write Modbus messages. In Modbus messaging, the Modbus client sends a request to the Modbus server. After receiving an indication, the Modbus server sends back a response to a Modbus client, which then receives a confirmation. In a standard Modbus network, there is a possibility to have one client and a maximum of 247 servers (Modbus Organization, 2006).

2.3.5 Sampling

As ADCs convert a continuous analog signal into digital value, they take samples from it several times per second reducing it into a discrete signal. The required sampling rate depends on the characteristics of the analog signal. The sampling rate must be sufficient in order to reconstruct the form of the original signal. Variables that have little variations over time or are practically in a steady state usually require sampling rates of only a few hertz (Measurement Computing, 2012). Some parameters in engine testing requires high-frequency acquisition, especially signals that are required to be recorded in the crank angle domain. The need for high sampling rates also sets the requirements for the sensor bandwidth, which describes the ability of a sensor to produce a rapidly varying signal (Osman & Massoud, 2013). According to Zhang et al. (2018), the required sampling rate for signals, that are recorded in the crank angle domain, depends on the engine speed and the resolution of the crank angle intervals. The sampling frequency of crank angle-based signals can be calculated with Equation (1)

$$f = \frac{360 \cdot N}{n \cdot 60}, \tag{1}$$

where N is the engine speed in rpm (revolutions per minute) and n is the resolution of the crank angle intervals.

In order to record all the information present in the signal, the Nyquist sampling theorem must be applied. According to the Nyquist sampling theorem, a signal must be sampled with a sampling rate of at least two times higher than the maximum operating frequency of the sensor. If the Nyquist theorem is not applied in sampling, an aliasing effect can occur. This means that the signal reconstructed from samples differs from the original continuous signal (Measurement Computing, 2012). Even if the signal is sampled at the frequency set by Equation 1, the effective resolution of the data also depends on the sensor bandwidth. In practical engine testing applications, it is good to have even higher sampling rate for crank angle-based data acquisition than the theoretical minimum stated in the Nyquist theorem. This enables confident reconstruction of the original signal that accurately represents the measured phenomenon (Zhang et al., 2014). The downside of a high sampling frequency is that it leads to large amounts of data. Therefore, sampling rates should not be unnecessarily high despite the recent developments in data storing technologies.

2.4 Combustion analysis and post-processing

ACT concepts like RCCI require precise shaping of the combustion process in order to provide superior efficiency and emission characteristics. Therefore, combustion analysis providing insight into in-cylinder phenomena is crucial for both, the fundamental understanding of the concept and its control on an applied level. The following section will

focus on the requirements of the measured parameters in order to perform the combustion analysis and the main results that are obtained. Particular attention is put towards special requirements set by the RCCI concept in question.

2.4.1 Combustion measurements

Conducting research on an internal combustion engine gives certain requirements for accuracies, resolution, and post-processing methods of measured parameters. As stated by Rogers (2010), cylinder pressure and crank angle are key parameters in measurements aiming to understand the combustion phenomenon occurring inside the cylinder. Depending on the purpose of the measurement, other parameters can also be measured. As discussed before, the piezoelectric pressure transducer is the most widely used instrument for measuring in-cylinder pressure due to its advantages and always requires proper amplification (Rogers, 2010). An angular encoder is used to measure crank angle reference at multiple points during a crankshaft revolution. When cylinder dimensions are known, the cylinder volume required in certain calculations can be derived from the angular position of the crankshaft (Heywood, 2018). After proper signal processing, sensor signals together with the encoder signal are sampled and digitized by the data acquisition system for further processing, displaying, and storing the data in the crank angle domain.

The measurement task defines the required resolution for the crank angle-based measurements. According to Rogers (2010) and Atkins (2009), basic calculations related to the combustion process and the direct analysis of a pressure curve are possible with a resolution close to 1 CAD (crank angle degree). On the other hand, some measurements like knock detection and combustion noise require resolutions down to 0.1 CAD.

Martyr and Plint (2012) divide the results of combustion analysis into two categories, direct and indirect results. Direct results, unlike indirect results, are acquired by analyz-

ing the raw data coming from measurement devices and do not require further calculations and post-processing. Results obtained specifically from the raw pressure curve include maximum pressure and pressure rise rate with respective angular positions. Additionally, abnormal conditions like knocking, misfiring, and combustion noise can be detected. In case of direct results, errors are similar in magnitude to the errors in measured signals. For calculated results, errors in measurements may lead to deviations by several orders of magnitude greater (Rogers, 2010). The measurement uncertainty for indirect results can be determined using the partial derivative method originally proposed by Kline and McClintock (1953). The uncertainty can be calculated with Equation (2)

$$\Delta Y = \left[\sum_{i=1}^{n}\left(\frac{\partial Y}{\partial x_i}\cdot \Delta x_i\right)^2\right]^{\frac{1}{2}}, \tag{2}$$

where Y is the calculated variable, x_i is the measured variable, Δx_i represents the error of the measured variable and n is the number of independent measurements used to calculate Y. The application of this method for engine uncertainty analysis can be found for instance in Mikulski et al. (2016).

2.4.2 Top dead center detection

Accurate alignment of the cylinder pressure curve in relation to the crank angle is important to mitigate errors in results and calculations. Alignment of the encoder is done by determining the angle difference between the top dead center (TDC) of the piston and the trigger mark of the angular encoder (Rogers, 2010). This difference is known as TDC offset and it defines how much the cylinder pressure curve has to be shifted in relation to crank angle. Rogers (2010) states that for some calculations, the determination of TDC position requires an accuracy of 0.1 CAD.

TDC can be determined with various methods. The manual way of TDC detection can be time-consuming and prone to errors (Rogers, 2010). The procedure requires a dial gauge to measure the distance of the piston from the TDC. The crankshaft is rotated approximately 90 degrees away from the TDC and the reading from the dial gauge is recorded. After this, the crankshaft is rotated in opposite direction as long as the piston distance indicated by the dial gauge equals the reading recorded previously. True TDC will be exactly in the middle of these two positions where piston height was equal according to the dial gauge (Rogers, 2010). After the TDC position has been determined manually, the encoder can be calibrated to trigger exactly at the TDC. According to Rogers (2010), the disadvantage of this method is that it does not consider that the actual TDC position may vary because some parts can change shape while the engine is running.

TDC can also be determined by reading the maximum value of the cylinder pressure curve (Martyr & Plint, 2012). According to Rogers (2010), assuming that cylinder peak pressure indicates TDC is not accurate enough, because thermodynamic loss angle specific to engine type and conditions needs to be considered. The main weakness of this method is the difficulty to accurately determine the thermodynamic loss angle. Typically, combustion measurement devices contain a specific built-in TDC detection procedure based on the method of pressure curve determination.

In addition to the methods described above, there is a possibility to use a specific type of capacitance sensor to accurately determine the TDC. The sensor needs to be mounted to a deactivated cylinder while the engine is running on the remaining cylinders. The sensor probe is located inside the cylinder and it measures the distance to piston crown. By using the data from the capacitive sensor and encoder, TDC can be determined with great accuracy (Rogers, 2010).

2.4.3 Zero-level correction

Because piezoelectric transducers are unable to measure the absolute cylinder pressure due to their dynamic response, zero-level correction (pegging) needs to be applied for further calculations and processing. In zero-level correction, the pressure curve obtained directly from the transducer is shifted on the Y axis according to a correction offset value (Δp) to have the curve represent the absolute cylinder pressure (Rogers, 2010). The simplest method of zero-level correction is to shift the whole cylinder pressure curve until it reaches the atmospheric pressure value at a reference point. According to Merker et al. (2012), this method has significant limitations because actual intake port pressure is not near atmospheric in the majority of modern engines.

One sufficiently accurate and fast method to determine the offset value is to calculate the thermodynamic zero-line correction value. In this method, two points from the pressure curve, are chosen before TDC and offset calculated with Equation (3)

$$\Delta p = \frac{\left(\frac{V_1}{V_2}\right)^{\gamma} \cdot p_1 - p_2}{1 - \left(\frac{V_1}{V_2}\right)^{\gamma}}, \tag{3}$$

where V_n and p_n represent cylinder volume and measured pressure at respective points of the curve, and exponent γ is the polytropic coefficient (Merker et al., 2012). The measured cylinder pressure curve is then shifted accordingly cycle by cycle. Calculation points which are not significantly affected by noise resulting from vibrations caused by intake valve motion must be chosen. Points with angle values from 100 CAD to 70 CAD before TDC are typically used (Rogers, 2010).

The zero-level correction that is based on a pressure value measured directly from the intake port is an accurate correction method. Correction offset is determined as a difference between the measured absolute intake port pressure and in-cylinder pressure value at a reference angle (Merker et al., 2012). The reference crank angle is usually the point at the bottom dead center (BDC) during intake valve opening where the piston speeds are the lowest, resulting in the lowest pressure gradients and oscillations. Care

needs to be taken that the reference point is outside the valve overlap or the valve closing phase. The two above requirements can be conflicting while advanced variable valve actuation strategies are incorporated. In such a case, more careful consideration of the reference is required. To mitigate the error resulting from noise, averaging the measured pressure values around the reference point should be used. To achieve the best accuracy, intake port pressure should be measured from every cylinder individually (Rogers, 2010).

2.4.4 Mean effective pressure

Mean effective pressure (MEP) is an important performance indicator of an internal combustion engine, which can be derived from the in-cylinder pressure curve plotted against cylinder volume, called as p-V diagram (Merker et al., 2012). Net indicated work (W_i) is a quantity that describes the work done by in-cylinder gas on a piston during the whole engine cycle and it can be calculated by integrating the enclosed area on the p-V diagram over the whole engine cycle, as shown in Equation (4)

$$W_{\mathrm{i}} = \oint p \, \mathrm{d}V, \tag{4}$$

where p is the cylinder pressure, and $\mathrm{d}V$ is the incremental swept volume (Heywood, 2018). Net indicated mean effective pressure ($\mathrm{IMEP_n}$) describes the ratio between the net indicated work and swept volume of the cylinder, as expressed in Equation (5)

$$\mathrm{IMEP_n} = \frac{W_{\mathrm{i}}}{V}, \tag{5}$$

where V is the cylinder swept volume (Heywood, 2018). Gross work is done on a piston during the working cycle and is calculated by taking the integration in Equation 4 over the compression and expansion strokes instead of the whole cycle (Martyr & Plint, 2012). Gross indicated mean effective pressure ($\mathrm{IMEP_g}$) is calculated by dividing the gross work by swept volume. As stated by Martyr and Plint (2012), pumping mean effective pressure

(PMEP) indicating the pumping losses during the gas exchange cycle can be derived from $IMEP_n$ and $IMEP_g$ with Equation (6)

$$\mathrm{PMEP} = \mathrm{IMEP_g} - \mathrm{IMEP_n}, \tag{6}$$

or by taking the integration in Equation 4 over the gas exchange cycle.

Due to mechanical losses and work necessary to drive auxiliary systems on a test bench, work delivered by the engine is always lower than indicated. Brake work of the engine can be expressed by using the brake power. According to Heywood (2018), brake work for four stroke engines can be calculated with Equation (7)

$$W_\mathrm{b} = \frac{2 \cdot P_\mathrm{b}}{N}, \tag{7}$$

where Pb is the brake power that the engine generates. From the calculated brake work, the brake mean effective pressure (BMEP) of the engine can be calculated using the Equation (8)

$$\mathrm{BMEP} = \frac{W_\mathrm{b}}{V}. \tag{8}$$

BMEP is an accurate indicator of engine's performance because it considers the losses. The friction mean effective pressure (FMEP) indicates the amount of work that is lost to friction. It can be derived from $IMEP_n$ and BMEP of the whole engine with Equation (9)

$$\mathrm{FMEP} = \mathrm{IMEP_n} - \mathrm{BMEP}. \tag{9}$$

According to Martyr and Plint (2012), accurate TDC detection is crucial for calculating the IMEP because even a 1 CAD difference between the encoder and true position of

the crankshaft will result to approximately 5% error in IMEP. For IMEP calculations, resolution for crank angle-based cylinder pressure data is required to be at least 1 CAD (Rogers, 2010).

2.4.5 Heat release rate

Heat release rate is a quantity in engine testing that indicates the energy released from the combustion (Heywood, 2018). Fundamentally, the cylinder pressure curve displays the in-cylinder pressure variations resulting from combustion, changing cylinder volume and heat transfer to surfaces (Rogers, 2010). Pressure variations with respect to volume can be derived from the polytropic coefficient and a change in volume. When the pressure variation due to changing volume is subtracted from the in-cylinder pressure curve, a curve resembling the net heat release can be derived with respect to crank angle degrees. Due to the strong correlation between heat release rate and in-cylinder pressure curve, accurate zero-level correction and TDC position are crucial in order to derive accurate heat release curve (Rogers, 2010). Heat release rate representing the rate of released energy during combustion minus heat absorbed to the walls and crevice volume is known as apparent or net heat release rate (Heywood, 2018). Multiple sources determine the net heat release rate based on the first law of thermodynamics with Equation (10)

$$\frac{\mathrm{d}Q_{\mathrm{net}}}{\mathrm{d}\theta} = \frac{\gamma}{\gamma - 1} \cdot p \cdot \frac{\mathrm{d}V}{\mathrm{d}\theta} + \frac{\gamma}{\gamma - 1} \cdot V \cdot \frac{\mathrm{d}p}{\mathrm{d}\theta}, \tag{10}$$

where θ is the crank angle and γ describes the composition of gas at a specific crank angle (Sogbesan, 2016; Willems et al, 2021). The gross heat release rate is obtained when heat losses are added to the net heat release rate (Heywood, 2018). Heat loss can be derived by calculating the rate of heat transfer between in-cylinder gasses and the cylinder wall with Equation (11)

$$\frac{\mathrm{d}Q_{\mathrm{ht}}}{\mathrm{d}t} \cdot \frac{1}{A_{\mathrm{cyl}}} = h_{\mathrm{c}} \cdot \left(T_{\mathrm{g}}^4 - T_{\mathrm{w}}^4\right) + \sigma \cdot \varepsilon \cdot \left(T_{\mathrm{g}}^4 - T_{\mathrm{w}}^4\right), \tag{11}$$

where A_{cyl} is the cylinder wall area, h_{c} is the heat transfer coefficient, σ is the Stefan-Boltzmann constant, ε is the emissivity, T_{g} is the temperature of the in-cylinder gas, and T_{w} is the temperature of the cylinder wall (Heywood, 2018). Therefore, the gross heat release rate is determined by Equation (12)

$$\frac{\mathrm{d}Q_{\mathrm{gross}}}{\mathrm{d}\theta} = \frac{\gamma}{\gamma - 1} \cdot p \cdot \frac{\mathrm{d}V}{\mathrm{d}\theta} + \frac{\gamma}{\gamma - 1} \cdot V \cdot \frac{\mathrm{d}p}{\mathrm{d}\theta} + \frac{\mathrm{d}Q_{ht}}{\mathrm{d}\theta}. \tag{12}$$

The cumulative heat release rate is calculated by integrating the gross heat release with respect to the crank angle from the closing of the intake valve to the opening of the exhaust valve (Willems et al., 2021). The curve of cumulative heat release indicates the amount of energy that has been released in relation to crank angle degrees. It enables one to derive the phasing of the 5%, 50%, and 90% of the total energy released, known as CA05, CA50, and CA90 respectively. Values of these parameters are important in RCCI control applications (Li et al., 2017). They are used in assessing ignition delay, and combustion phasing, as well as in monitoring the effect of input variables on the rate of combustion (Sogbesan, 2016). Combustion duration can also be derived from the cumulative heat release curve (Heywood, 2018).

During heat release rate calculations, the polytropic coefficient, γ, is often assumed constant, while in reality it varies due to several factors such as heat transfer to the walls, in-cylinder gas composition, and valve timing (Lee & Min, 2019). The problem with using a constant polytropic coefficient in RCCI is that it can vary significantly between different operating points due to above-mentioned reasons. More accurate estimation of the polytropic coefficient is crucial when developing and using advanced combustion concepts, such as RCCI (Rogers, 2010).

Rogers (2010) states that the calculation of heat release rate in commercial combustion measurement systems is typically computed with a simplified process resulting in net heat release. The calculated value is approximately 20% lower than the gross heat release due to ignored surface and blow-by losses. Error in the result is more significant towards the end of the combustion process. Simplified calculation may be required if repeatability is more important than the high level of accuracy and when processing capacity is of concern. As discussed above, accurate determination of heat release rate and thus cumulative heat release rate in RCCI applications are particularly important in understanding the combustion phenomenon and enabling its efficient control. Therefore, the use of any simplified process should be critically assessed. For heat release calculations, a resolution of at least 1 CAD should be used, and although finer resolution improves the accuracy, it can significantly increase processing time (Rogers, 2010).

2.4.6 Gas exchange analysis

The gas exchange process is part of the engine cycle where exhaust gases are forced out of the cylinder and a fresh mixture of air is drawn from the intake port. Gas exchange analysis offers a thorough understanding of the phenomena during this event and has significant importance in modern engine research and development. According to Rogers (2010), pressure measurements from intake and exhaust manifolds provide information to optimize gas exchange processes and accurately calculate the PMEP, which together with BMEP allows a more precise evaluation of friction losses.

Measuring absolute intake port pressure during the gas exchange process also allows accurate estimation of in-cylinder air flow. According to Ferguson & Kirkpatrick (2015), the mass flow rate through the valve is determined with Equation (13)

$$\frac{\mathrm{d}m}{\mathrm{d}t} = \rho_{\mathrm{v}} \cdot A_{\mathrm{eff}} \cdot U_{\mathrm{is}}\,, \tag{13}$$

where ρ_v is the fluid density at the valve, A_{eff} is the effective valve area, and U_{is} is the reference isentropic fluid velocity. Reference isentropic velocity is affected by the ratio of in-cylinder pressure to intake port pressure near the valve. Reference isentropic velocity can be calculated with Equation (14)

$$U_{is} = \sqrt{R \cdot T_{in}} \cdot \left[\frac{2 \cdot \gamma}{\gamma - 1} \cdot \left(1 - P_r^{\frac{\gamma - 1}{\gamma}} \right) \right]^{\frac{1}{2}}, \tag{14}$$

where R is the gas constant for intake gas, T_{in} is the intake temperature and P_r is the pressure ratio of in-cylinder pressure and intake port pressure (Ferguson & Kirkpatrick, 2015). The use of a constant polytropic coefficient in air flow calculations is more justified than in heat release rate calculations due to steadier conditions. Calculating the air flow rate entering the cylinder allows more accurate estimation of in-cylinder gas composition and temperature at intake valve closing. Both parameters are further crucial for an accurate determination of the in-cylinder polytropic coefficient and in-cylinder temperature.

According to Rogers (2010), in order to measure intake and exhaust pressures accordingly, transducers capable of measuring absolute pressure are mounted as near as possible to the valves. Absolute pressure measurements are a prerequisite for zero-level correction via intake port pressure measurements. Transducers installed in the manifolds, especially on the exhaust side, often face more issues concerning vibration and extreme temperatures than those measuring in-cylinder pressure. Resulted noise may introduce significant errors in the measured pressure curves due to the relatively low range of the signal. Therefore, manifold pressure measurements require transducers that exhibit characteristics like stable output signal during high-temperature shifts, resistance to vibrations and accuracy, especially when used for determining the zero-level correction (Rogers, 2010).

3 Objects and methods

3.1 VEBIC W4L20 engine test cell

The thesis work considered the improvement of the measurement and data acquisition system in the large-bore engine test cell located in the VEBIC laboratory. The test cell is used to operate a medium-speed 4-stroke Wärtsilä 20 diesel engine. During CPT project, cylinder 4 is modified to allow RCCI combustion. Detailed instrumentation regarding the RCCI test bench will be discussed in chapter 3.2. The basic layout of the engine test cell, disregarding the instrumentation and systems specific to cylinder 4, is shown in Figure 14. However, the exhaust path and the fuel line are drawn according to modifications. Detailed insight regarding the baseline test bench, before implementing the outcomes of the CPT project and this thesis, is provided in several publications (Hautala et al., 2022; Söderäng et al., 2022).

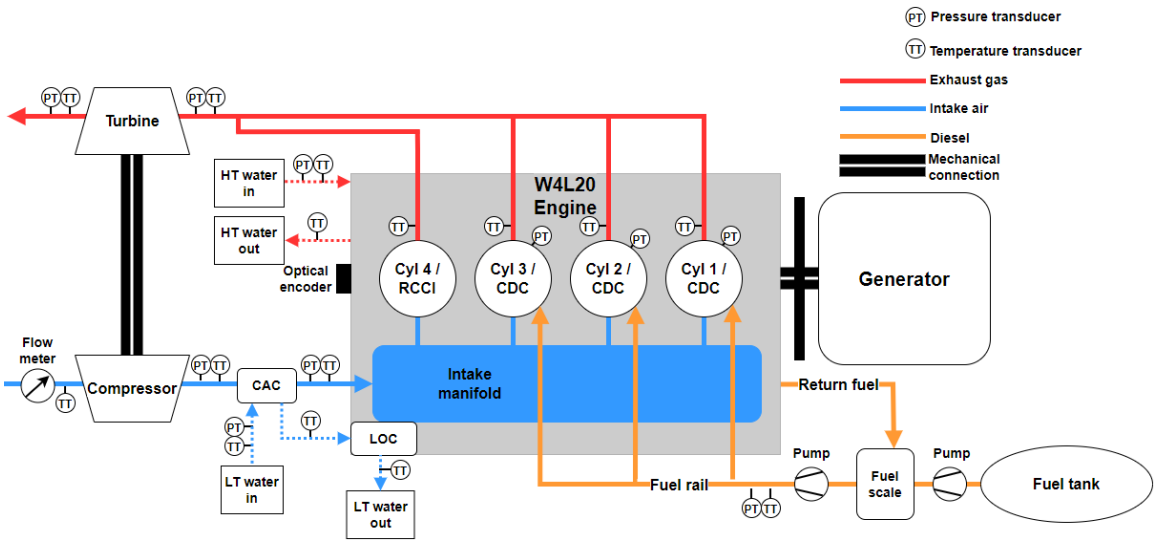

Figure 14. VEBIC W4L20 engine test cell.

3.1.1 Engine overview

The Wärtsilä 4L20 engine located in the VEBIC test cell is a turbocharged 4-cylinder direct injection diesel engine that can be used in marine or electricity generation applications. During the CPT project, the engine has 3 cylinders that remain unmodified and operate in CDC mode. The cylinder that operates in RCCI mode is located furthest from the flywheel, as illustrated in Figure 14. The mechanical energy of the crankshaft is converted into electrical energy through ABB M3LG 450LC, a squirrel cage induction generator rated at an output power of 1050 kW. Produced electricity can be fed to the grid. Table 1 depicts the main data of the Wärtsilä 4L20 engine, before the retrofit.

Table 1. Wärtsilä 4L20 engine specifications.

Engine	Wärtsilä 4L20
Cylinder configuration	4-cylinder, inline
Bore diameter [mm]	200
Stroke [mm]	280
Connecting rod [mm]	510
Displacement per cylinder [dm^3]	8.8
Compression ratio	15.8:1
Number of valves per cylinder	4

3.1.2 Fuel system

VEBIC engine laboratory has 3 fuel tanks to store different liquid fuels. There are two tanks for fuel oil that have a capacity of 25 m^3 and one tank for bio-oil that has a capacity of 10 m^3. The test cell has two 300-liter day tanks that can be used during engine operation instead of the main tanks. A schematic of the fuel system can be seen in Figure 14. A transfer pump is used to move the fuel from a tank through an automation filter into a 30-liter weight tank that is used in liquid fuel consumption measurement. Fuel is then pumped from the weight tank into a mixing tank. A booster pump feeds fuel from the mixing tank to the common rail injection system with high pressure. Pressure and temperature are measured from the fuel rail using a strain gauge and an RTD respectively.

Fuel is injected into cylinders from a common rail injection system and possible spillback fuel is returned to the weight tank.

3.1.3 Intake and exhaust system

The engine is equipped with an ABB TPS48E01 turbocharger (Hautala et al., 2022). The turbocharging system compresses the air entering the engine. Compressed intake air goes to the intake manifold through a charge air cooler which cools the air down. Compressed and cooled air is drawn inside the cylinder through intake valves. Sensyflow FMT700-P flow meter measures the turbocharger blow by from the intake side (Hautala et al., 2022). Temperatures from the turbocharger inlet and intake manifold are measured using RTDs, while temperature before the charge air cooler is measured with a K-type thermocouple. Intake air pressure is measured before the cooler and from the intake manifold with strain gauge transducers.

After the combustion, exhaust gases flow through the exhaust valves into the exhaust pipe and spins the turbocharger turbine driving the compressor. The exhaust pipe from cylinder 4 is isolated in order to prevent the exhaust gases from other cylinders from interfering with the measurements from cylinder 4. From Figure 14 can be seen that temperature is measured from the exhaust port of each cylinder. Temperature and pressure from the whole exhaust stream are measured before and after the turbine. K-type thermocouples are used in every exhaust system-related temperature measurement.

3.1.4 Cooling and lubrication system

The cooling system of the engine consists of two independent cooling circuits as seen in Figure 14: high temperature (HT) and low temperature (LT) water circuits. Both circuits are powered by their own pumps located at the free end of the engine and they are driven by gears connected to the crankshaft. The cylinders and cylinder heads are cooled

with the HT circuit. Temperature is measured from the inlet and outlet of the HT circuit, while pressure is measured from the inlet side. LT circuit goes through charge air cooler and lubricating oil cooler, providing cooling for intake air and lubricating oil respectively. Similar to measurements taken from the HT circuit, the temperature of the LT circuit is measured from both the inlet and outlet, while the pressure is measured from the inlet side only. Temperature is also measured after each cooler. All temperatures from the cooling system are measured using RTDs.

Lubricating oil is pumped from the oil sump with a pump driven by crankshaft-connected gears at the free end of the engine. From the sump, oil circulates through the components requiring oil and lubrication. Lubricating oil flows back to the oil sump through the cylinder liner. Before start and stop procedures, the engine requires pre-lubrication provided by an externally-powered pre-lubricating pump. Lubricating oil temperature is measured before and after the engine with RTDs, while pressure is measured from various places like before the engine, the oil filters and the turbocharger.

3.1.5 Control system

The test cell control system is based on ABB AC800M PLC, which is responsible for controlling the test cell subsystems. The PLC is also used to align the engine and generator operation at a given load. In the test cell, ECU functionalities of the Wärtsilä 4L20 engine are implemented on a Speedgoat real-time target machine suitable for RCP and HIL testing. The Speedgoat is equipped with multiple I/O (input and output) modules that are used in controlling combustion and injection parameters for optimized engine performance at a specific operating point. The Speedgoat is operated through CANape, which is a calibration and monitoring software. The communication interface between the PLC and the Speedgoat is based on Modbus TCP/IP protocol, where the PLC acts as a client. Additionally, the Speedgoat communicates through Modbus with a computer that includes the digital twin of the engine coupled to a power plant model (Söderäng et al., 2022).

3.2 RCCI engine test bench instrumentation

As discussed before, major modifications were done to cylinder 4. The extent of these modifications and the instrumentation will be discussed in the next sections. Schematic of the cylinder 4 and related instrumentation are depicted in Figure 15 below.

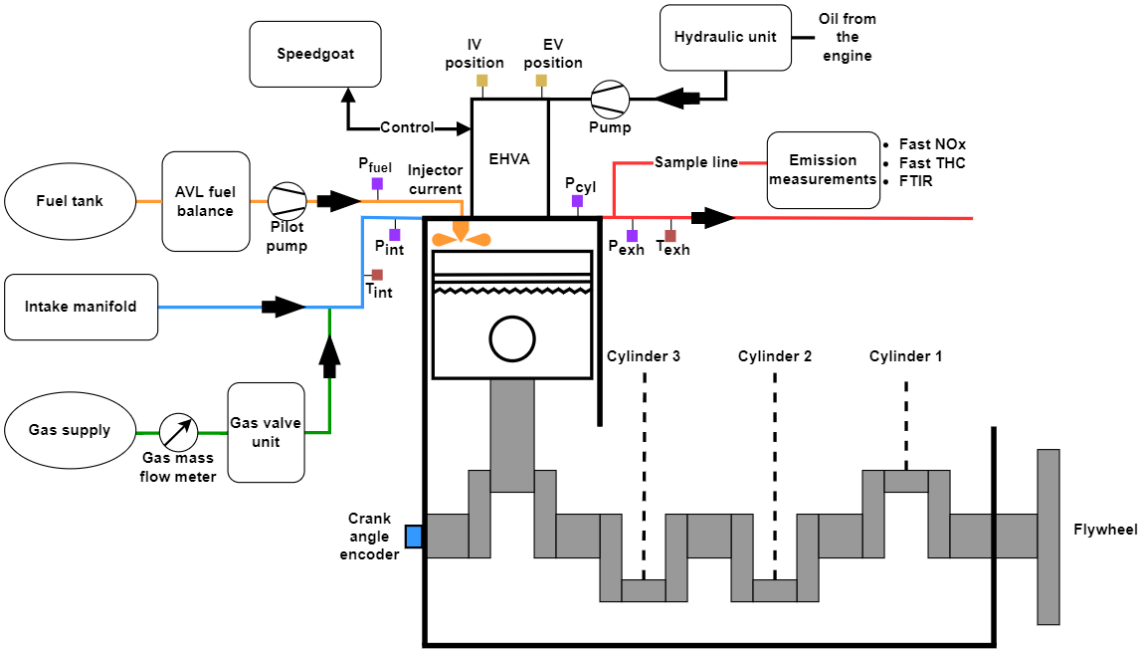

Figure 15. Instrumentation of the RCCI cylinder.

In order to enable RCCI operation, cylinder 4 was converted to a dual-fuel by building a natural gas supply infrastructure and a separate pilot fuel line to the cylinder. Natural gas is injected through the common rail pipe into a duct where it mixes with air before entering the cylinder. The RCCI cylinder is equipped with its own pilot fuel pump which enables high-pressure injection of diesel directly into the combustion chamber. The common exhaust pipe of the engine was disassembled and replaced with new exhaust piping. The design of the new exhaust piping allows the decoupling of cylinder 4 from CDC cylinders. The new exhaust line consists of two separate pipes that connect at the turbo-

charger, as illustrated in Figure 14. The new air path is provided with its own, detail instrumentation and separating the exhaust paths from each other ensures that the emission measurements taken from RCCI cylinder are not compromised by the disturbance from other cylinders. Additionally, valves of the cylinder 4 were disconnected from the camshaft and an electro-hydraulic valve actuation (EHVA) developed by Wärtsilä was installed. It enables fully variable valve timing and valve lifts for cylinder 4. The functionality is considered one of the enablers for efficient RCCI combustion throughout the operating range. This work focuses on providing the RCCI cylinder and related subsystems with proper instrumentation in order to enable necessary measurements. In Table 2, characteristics of the measurement instruments specific to the cylinder operated in the RCCI mode are presented.

Table 2. Specification of measurement instruments used in the RCCI cylinder.

Measurement application	**Instrument**	**Range**	**Accuracy (-) / Linearity error (L)**
Crank angle	Kistler 2614CK	0–12000 rpm	<0.0012 °
In-cylinder pressure	Kistler 6613CG1	0–250 bar	<±0.5 % FSO (L)
Intake port pressure	Kistler 4007D	0–10 bar	<±1 % FSO
Exhaust port pressure	Kistler 4049B	0–10 bar	<±0.3 % FSO
Piezoresistive amplification	Kistler 4624AK	-	<±0.5 % FSO
Intake air temperature	Nokeval PT2T	-50–250 °C	-
Exhaust air temperature	-	-	-
Fuel injection pressure	Trafag 8298	0–2500 bar	<±0.5 % FSO
Injector current profile	Fluke 80i-110s	0–10 A	<± (3 % RD+50mA)
Valve position	Positek P846	0–20 mm	<±0.2 % FSO
Pilot fuel consumption	AVL fuel balance	0–150 kg/h	<±0.12 % FSO
Gas mass flow	Micro Motion F025S	0–190 kg/h	<±0.5 % FSO
FTIR analysis	Gasmet DX4000	-	<±2 % FSO
Fast NOx measurement	CLD500	8 selectable	<±1 % FSO (L)
Fast THC measurement	HFR500	8 selectable	<±1 % FSO (L)

In Table 2, accuracies are given as a percentage of the full-scale output (% FSO). In the case of the cylinder pressure transducer and fast emission analyzers, the accuracy is given as a linearity error. Linearity error describes the percentage that the actual output deviates from the ideally linear output (Rogers, 2010). In the case of the Fluke 80i-110s current probe, accuracy is specified as a percentage of reading (% RD) and additional

uncertainty considered. There are eight measurement ranges selectable for the fast emission analyzers. Ranges from 0–100 ppm to 0–20000 ppm are available for CLD500 and ranges from 0–1000 ppm to 0–200000 ppm are available for HFR500 (Cambustion, 2008; Cambustion, 2004). The devices and systems essential to the objectives of the work are discussed in the following subsections.

3.2.1 Electro-hydraulic valve actuation (EHVA)

EHVA is used to control the intake and exhaust valves of cylinder 4. The main components of the system in addition to intake and exhaust valves are the control unit, control valves, analog signal converters, and linear position sensors. The control of EHVA is implemented on a Speedgoat, which is a separate unit from the main Speedgoat that is used in engine control. The EHVA Speedgoat communicates with the main Speedgoat via CAN communication, through which it gets the engine speed reference. During operation, the Speedgoat sends a control signal to Parker D3FP proportional directional control valves, which allows for hydraulic oil to flow through the control valve and push the valves open. The hydraulic oil pressure is generated with a separate electric motor-powered hydraulic unit which draws the oil from the engine's oil sump. The control valves require a current signal to operate. Because the analog output (AO) card of the Speedgoat has a voltage output, it is converted into a current signal via ABB CC-E/STD analog signal converter.

3.2.2 Crank angle encoder

Kistler 2614CK crank angle encoder is used to provide a reference for crank angle and full revolutions for the data acquisition system. The encoder is mounted to the free end of the crankshaft. There are 720 uniformly distributed marks in the encoder's marked disc which means there is a pulse every 0.5 CAD (Kistler, 2016). There is also another row

in the disc with a single mark that outputs one pulse per revolution. The encoder is connected to Kistler's encoder electronics type 2614C21 which is used for signal processing. Encoder electronics has two types of outputs representing the encoder output. The low-voltage differential signal and transistor-transistor logic (TTL) signal are both pulse wave-shaped signals and can be used depending on compatibility with the data acquisition system that is sampling the signal. Encoder electronics requires a power supply from 5 VDC to 30 VDC to operate.

3.2.3 High sampling frequency measurement instruments

In-cylinder pressure of each cylinder is measured with Kistler 6613CG1 piezoelectric pressure transducer that includes an in-line amplifier. The transducer has an output of 4–20 mA with a measuring range from 0 to 250 bar, giving the transducer a sensitivity of 0.05 mA/bar (Kistler, 2018). This transducer is also suited for closed-loop combustion control applications, which is a requirement for this RCCI test bench.

Intake port pressure is measured with a piezoresistive Kistler 4007D absolute pressure transducer. The transducer is mounted close to the intake valves and is able to withstand operating temperature of up to 200 °C without the need for additional cooling. In the application of port pressure measurements, Kistler 4007D with a measuring range from 0 to 10 bar is used. The signal from the transducer is conditioned with a Kistler 4624AK piezoresistive single-channel amplifier. Measurement of exhaust port pressure is done with a water-cooled Kistler 4049B piezoresistive absolute pressure transducer. The transducer is mounted near the exhaust valves and can operate in temperatures of up to 1100 °C. The transducer has a measuring range from 0 to 10 bar and Kistler 4624AK piezoresistive single-channel amplifier is used for signal conditioning.

Injector current profiles are measured with Fluke 80i-110s AC/DC current probe based on Hall effect. A separate probe measures the excitation current of the cylinder 4 injector. The probe has a clamp that is wrapped around the injector cable, through which the

waveform of the injector current is reproduced as a voltage output. There can be two different sensitivities selected for the output signal depending on the amplitude of the measured current. Because the amplitude of the injector current is less than 10 A, the sensitivity of 100 mV/A is used (Fluke, 2017).

There are two Positek P846 linear position sensors mounted on top of the EHVA that measure the lifts of the valves and provide real-time valve position feedback for the EHVA's control unit. The operation of the sensors is based on the working principle of common inductive position transducers. The sensors measure absolute valve position up to 20 mm and produce an output of 4–20 mA, which is linear to the lift. This gives the sensor sensitivity of 0.8 mA/mm. Additionally, gas exchange valve control signals from the Speedgoat AO card are measured in the crank angle domain.

3.2.4 Low sampling frequency measurement instruments

Low sampling frequency temperature and pressure measurements are mainly needed in system monitoring and control applications. For exhaust gas temperature measurement, a K-type thermocouple is mounted to the exhaust port. Intake air temperature is measured directly from the intake port with a 4-wire Nokeval PT2T sensor, which is a Pt-100 RTD. Trafag 8298 strain gauge pressure transducer is mounted to the pilot fuel line for pressure measurement. Every low sampling frequency temperature and pressure sensor that was already installed in the test bench before the modifications remain the same.

3.2.5 Fuel consumption measurement system

The RCCI cylinder has two fuel supply systems that are separate from the fuel system of other cylinders. Consumption of pilot fuel that ignites the fresh mixture inside the cylinder will be measured with AVL fuel balance, which is a gravimetric fuel scale. The device has a weighing container that is linked to a hydraulic damper with a measuring beam. A

capacitive sensor tracks the movement of the beam caused by decreasing weight of the container. The mass of the consumed fuel is derived from the output of the sensor with a measurement frequency of 10 Hz. The AVL fuel balance needs to be mounted rigidly on the wall to minimize the vibrations that could potentially introduce additional errors to the measurement. Recommended measuring range for the fuel scale is from 0 to 150 kg/h and it communicates with its software via the RS-232 interface. The mass flow of the natural gas is measured with a Micro Motion F025S Coriolis mass flow meter connected to the PLC. The meter is located before the gas valve unit and has a maximum recommended flow rate of approximately 190 kg/h at 10 bar, which is the maximum operating pressure for the gas valve unit.

3.2.6 Emission measurement system

In order to take emission measurements from the exhaust port near the valve, a pressure-reducing unit is needed to reduce the pressure of exhaust gas going to the analyzers. After reducing the pressure, the sample line is divided between three analyzers that are used to measure emissions from the exhaust port. FTIR measurements from the exhaust gas are carried out via the Gasmet DX4000 FTIR gas analyzer. To convey the sample gas to the FTIR analyzer, an electrically heated PSP4000-H sampling probe is connected to the pressure-reducing unit preventing the sample gas near the sampling point from cooling and condensing. From the sampling probe, sample gas goes to the Gasmet portable sampling unit, which is used to pump the sample gas from the sampling point. The sampling unit measures the O_2 concentration from the sample gas via ZrO_2 principle and sends the information through the analyzer. After the sampling unit, the sample gas is directed into the FTIR analyzer that is connected to an external computer through RS-232 interface.

Direct measurements taken from the port will also include fast response NO_x and THC measurements. Fast response measurements enable crank angle-based NO_x and THC

data. Analyzers that will be used to provide these fast response measurements are Cambustion CLD500 fast NO_x and HFR500 fast FID analyzers. In both of these analyzers, the detector is located in the sampling head near the sampling point. The sampling head is connected to a control unit via a 10-meter-long conduit inside of which are necessary connections for the detector. The vacuum pump draws the sample gas into the detector through a heated probe. Because detection happens near the sampling point, fast response times can be achieved for NO_x and THC measurements. It should be noted that the location of the sample probe is crucial to minimize the time delay resulting from the sample travelling into the sampling system. The sample head of CLD500 can be equipped with a NO_x converter that enables the measurement of NO_2 in the sample gas as well, although it increases the response time (Cambustion, 2008). As stated in the literature review, the CLD principle utilizes the light produced in the reactions of ozone and NO. This is why the converter needs to reduce the NO_2 in the sample gas into NO before it can be measured by the detector. Both analyzers are connected to their own control software via RS-485 interface and provide an analog output signal from 0 to 10 VDC (Cambustion, 2008; Cambustion, 2004). Figure 16 represents the intended exhaust gas sampling setup in the RCCI test bench more precisely. It shows the layout with the pressure-reducing probe, sampling system and analyzers. Red arrows indicate the direction of the exhaust flow and blue lines represent the conduits connecting the sampling heads of the fast response emission analyzers to the control units.

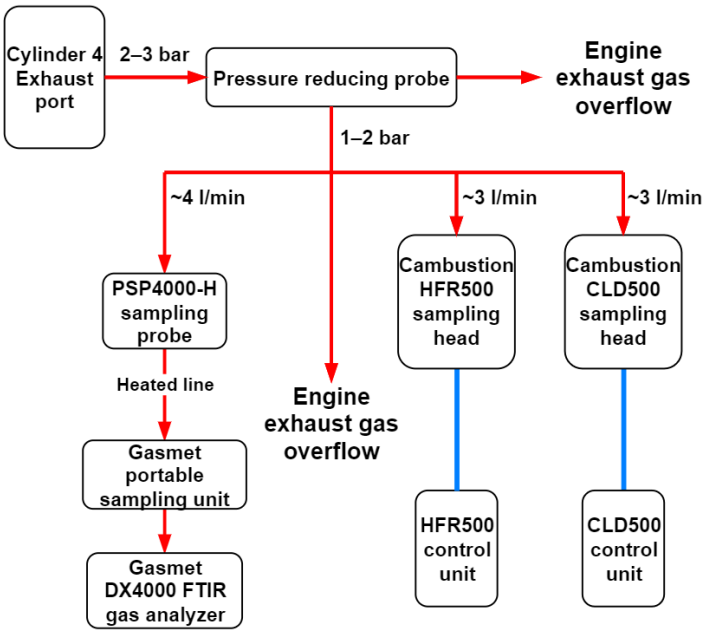

Figure 16. Structure of the intended exhaust gas measurement system of the RCCI cylinder.

3.3 Data acquisition

The data acquisition system collects data coming from different measurement instruments and analyzers. The data is used for monitoring and analyzing the operation of the engine and related subsystems, as well as in control applications. The data acquired during engine operation can be divided into two categories, low-frequency and high-frequency data. Because the goal of this thesis is to provide W4L20 engine test bench with a new data acquisition system enabling RCCI research, it is important to understand the status of the data acquisition system before the new system is designed and implemented. The subchapters below are dedicated to describing the state of the data acquisition system prior to modifications.

3.3.1 High-frequency data acquisition system

Before the CPT project, in-cylinder pressures were sampled at 0.1 CAD resolution and analyzed via the Kistler KiBox combustion analysis system. An injection excitation current

from one cylinder was also acquired via KiBox. The KiBox was connected to a laptop equipped with KiBox Cockpit software through ethernet connection. The software was used to configure the input channels, perform combustion analysis, as well as display and store the data. The KiBox previously used in the test cell has 8 analog input channels for voltage signals ranging from 0 to 10 VDC. The functionality of the original system was considered insufficient for the purpose of advanced analysis planned in the CPT project. In this thesis, a 16-channel Dewesoft SIRIUS data acquisition system is implemented and integrated into the existing test bench data acquisition system to replace the KiBox. In Table 3, the main characteristics of both systems are specified.

Table 3. Comparison of Kistler KiBox and Dewesoft SIRIUS data acquisition systems.

System	Analog channels	Input voltage range [VDC]	ADC resolution [bit]	Maximum sample rate per channel [kHz]
Kistler KiBox	8	0–10	16	310
Dewesoft SIRIUS	16	0–50	24 (Dual Core)	200

The design and implementation of the Dewesoft SIRIUS based data acquisition system will be discussed in detail in chapter 4. It can be noted that the Dewesoft data acquisition system offers several advantages compared to the previously used KiBox. There are more input channels, the system is more affordable and enables more efficient integration with the low-frequency data acquisition system. In addition, the Dewesoft system can be expanded relatively easily and inexpensively compared to the KiBox.

3.3.2 Low-frequency data acquisition system

Pressure transducer signals coming from the engine are sampled via input modules of the main Speedgoat and used for engine control. Thermocouple and RTD measurements are acquired through data loggers that communicate through Modbus TCP/IP interface with the main Speedgoat. System related safety signals are acquired through PLC input modules. Additionally, the fuel balance of the test cell is operated and data is acquired

through the PLC. The PLC and main Speedgoat communicate with each other and send signals related to the engine and subsystems through the Modbus TCP/IP network. Data collection was previously carried out by the common data acquisition system that recorded the signals at a frequency of approximately 1 Hz and saved them on a computer hard drive. The FTIR measurements from the Gasmet DX4000 FTIR analyzer and O_2 concentration measured by the sampling unit were logged to the channels of the Calcmet software used to operate the FTIR analyzer. From there, the data could be saved to a local data storage of the computer. Figure 17 illustrates the layout of the test cell data acquisition system prior to the CPT project.

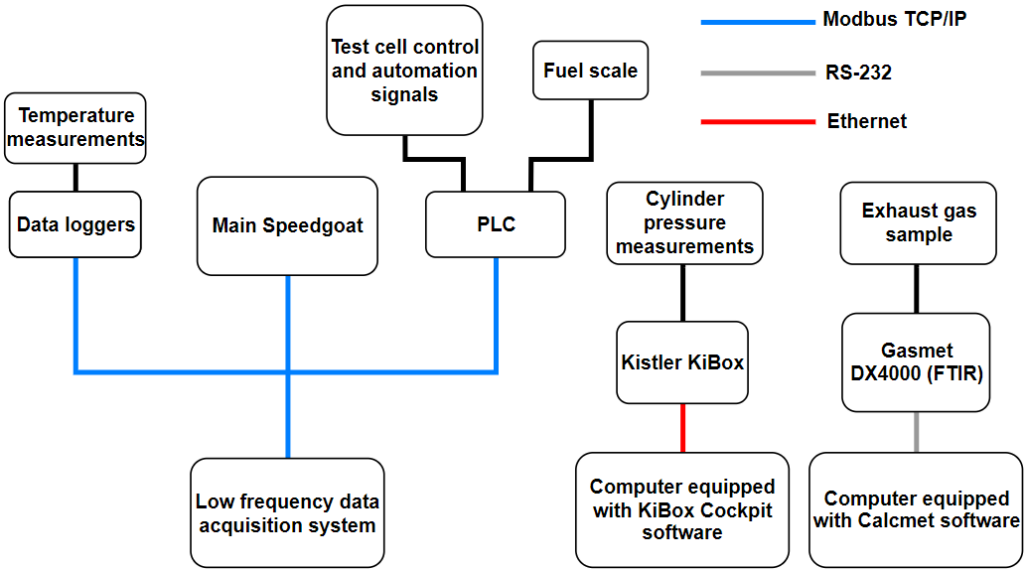

Figure 17. The layout of the W4L20 engine test cell data acquisition system prior to modifications.

3.4 System design and validation methodology

This section describes the methodology regarding the design phase of the data acquisition system. Methods to ensure system performance and proper operation, as well as the validity of the measurements and data, are also discussed.

3.4.1 System design

System design is based on meeting the requirements for the test bench data acquisition system. The system designed in this work will include multiple different measuring instruments, data acquisition hardware, and software each having its own specifications and output signal types. In order to design a robust system that meets the requirements, knowledge of the test cell system before modifications is required. Related literature and manuals provided by suppliers are studied and physical testing of individual devices and subsystems is carried out during the design process.

As stated before, errors are always present to some extent in a measurement system. However, proper system design and implementation will reduce the impact of environmental interference. Errors resulting from the analog signal transmission are mitigated by using shielded cables and installing them as far from interference sources as practically possible while maintaining short distances. General methods to reduce measurement errors have been discussed in detail in chapter 2.3.2.

3.4.2 Performance validation

The quality of individual instruments used in a measurement chain contributes positively to overall system performance. For example, selecting modern, high-grade pressure transducers will significantly reduce the effect of sensitivity drift resulting from temperature variations of the transducer over time. This is due to improved design and manufacturing methods of modern transducers (Rogers, 2010). Systematic measurement uncertainty calculation for the high-frequency analog signal acquisition will be done as a part to validate the accuracy of the system. According to Morris and Langari (2012), systematic measurement error can be calculated by using a root-sum-squares method. With this method, error E is determined by Equation (15),

$$E = \pm \sqrt{\sum_{j=1}^{n} x_j^2} \ , \tag{15}$$

where x_j is the systematic error component of the measurement chain. The level of system integration is also a part of the system's performance. Error calculations will be discussed in chapter 5.

At the time of the thesis, W4L20 engine cannot be started up due to ongoing hardware and automation system modifications. Therefore, the data acquisition system cannot be validated entirely. However, the system will be validated by performing an EHVA unit test. This enables the validation of crank angle-based measurement, monitoring and data storage.

3.4.3 System prechecking

Verifying connections between the measurement instrument must be made before starting the measurements. In the case of most signals, this can be verified by checking that the sensor or transducer produces a value on the monitoring interface. Most of the transducers are designed to produce a signal even at the lower end of the measurement range. Mounting the instrument properly is crucial to ensure that the sensor element is properly in contact with the measured object. Also, improper mounting of highly sensitive pressure transducers, especially those measuring the in-cylinder pressure, will cause vibrations to significantly affect the measurements and post-processing results derived from them (Rogers, 2010). Calibrating all instruments in the measurement chain according to manufacturer instructions ensures that the performance of the instruments is in line with manufacturer specifications. Before each measurement campaign, the validity of measurement device calibrations needs to be verified and if necessary, calibration of the instruments is required. Calibration is carried out by comparing the outputs of the measuring instrument used in testing and a measuring instrument of known accuracy

when the same input is given to both instruments. The calibration procedure is performed at multiple measurement points covering the whole measuring range of the instrument. The number of calibration points depends on the measuring instrument and the desired accuracy of the calibration (Morris & Langari, 2012). In the case of emission analyzers, a calibration gas that has a known composition and concentrations of the measured compounds close to the expected amounts is passed through the analyzer (Nakamura & Adachi, 2013). Depending on whether the output of the instrument under calibration deviates from the output of the other instrument, proper adjustment to the offset is applied to ensure that the possible deviation is considered during measurement. If signs of instrument damage are noticed during calibration, repairing or changing the instrument is required. The principle of calibration methodology is the same for a large variety of different measurement instruments. Required calibration frequency, on the other hand, varies between different instruments. It is difficult to determine properly, because it depends on many factors, such as the type of instrument and measurement conditions (Morris & Langari, 2012).

3.4.4 Reference measurements

Validation of the measurements should be made before, during and after each measurement sequence by monitoring the data curves and calculated results. Reference measurements during a test program at the specific reference operating point is stated by Rogers (2010) to be an effective data validation method. These measurements should be made regularly and the most important parameters need to be statistically represented. Statistical analysis is a powerful tool in system validation because relatively large and sudden variations in parameters indicate that there is a problem in the system that needs to be solved. The main statistical tools used to validate the measurements are average, standard deviation, and covariance. Calculating the average of the most important parameters and comparing them to previously made measurements, it can be quickly verified whether the performance of the system has remained the same. According to Rogers (2010), peak pressure-related results, as well as average IMEP values over

the test sequence, are a good measure for describing the repeatability of the measurements. Standard deviation is used to examine how individual measurement values are distributed with respect to mean value (Morris & Langari, 2012). Standard deviation, σ_s, of measured values is calculated with Equation (16)

$$\sigma_s = \sqrt{\sum_{i=1}^{n} \frac{(x_i - \overline{x_i})}{n-1}}, \tag{16}$$

where x_i is the measured value and n is the number of values during the measurement. The standard deviation of IMEP and the standard deviation of engine speed are used to quantify cycle-to-cycle variability (Atkins, 2009). In addition, the covariance of IMEP is a good measure of cyclic variability derived from cylinder pressure data. Covariance of IMEP is calculated with Equation (17)

$$\mathrm{COV}_{\mathrm{IMEP}} = \frac{\sigma_{\mathrm{IMEP}}}{\overline{\mathrm{IMEP}}} \cdot 100\%, \tag{17}$$

Where the standard deviation of IMEP is divided by the mean IMEP and converted to a percentage (Heywood, 2018). Frequent and thorough reference measurements and statistical analysis enable more efficient problem identification and solving.

4 System design and implementation

This section discusses the data acquisition system design and implementation that was carried out during this thesis. Chapter 4.1 discusses the overall requirements for the W4L20 engine test bench data acquisition system to enable RCCI research. This acts as a background for the later chapters that focus on the implementation of the system. Chapter 4.2 includes a detailed description of the data acquisition system chosen based on the requirements. Additionally, the installation of the most important devices, as well as sensor and analyzer connections to the data acquisition system is described. In chapter 4.3, the configuration of the data acquisition system is discussed. It explains how the channels of the data acquisition hardware were configured and what was done to enable high-frequency data to be recorded and monitored in the crank angle domain, including related data post-processing and real-time calculations. The integration of the W4L20 test cell automation and control system with the data acquisition system is discussed. Additionally, monitoring and data storing functionalities of the data acquisition system are described.

4.1 System requirements

Figuring out the requirements for the measurement system enabling RCCI research on the W4L20 engine is crucial in order to choose a proper data acquisition hardware for the task. The data acquisition system designed and implemented in this thesis has to be able to record both, high-frequency measurements and low-frequency measurements simultaneously. In the RCCI test bench located in VEBIC, a total of 14 signals are required to be recorded in reference to crank angle. The nominal rotational speed of the Wärtsilä 4L20 engine is 1000 rpm, which corresponds to a sample rate of 60 kHz for crank angle-based signals at a 0.1 CAD resolution according to Equation 1. As discussed in the litera-

ture review, data acquisition system must be capable of sampling crank angle-based signals with at least two times the expected sample rate to satisfy the criterion set by the Nyquist theorem.

The answer to the first research question set in the thesis, concerning system requirements for LTC research, is the following. The engine test bench data acquisition system in VEBIC needs to be able to acquire and process the data coming from the measurement devices installed to the test bench, as well as perform necessary calculations for post-processing in real-time. In order to do this, the data acquisition system must acquire the crank angle-based high-frequency measurements, as well as the measurement data that comes through the Modbus TCP/IP network of the test cell. Due to many channels with high sampling frequencies, the engine measurement system outputs a large amount of data during measurement. To ease the data management, the files created are required to be named logically. Monitoring the operation of the engine is an important task related to the test cell measurement system. The engine monitoring interface needs to be flexible in order to be optimized for a specific test procedure and customized according to the preference of the person in charge of monitoring. From monitoring system, parameters are constantly monitored and checked to notice possible abnormal behavior, such as cyclic variability of the combustion parameters. The data acquisition system chosen to fulfil the requirements regarding measurement, data recording, and monitoring tasks was Dewesoft SIRIUS data acquisition hardware, which will be discussed more in chapter 4.2.

4.2 Device installations and connections

Establishing device installations and connections is part of the second research question about integrating different measuring instruments into a common data acquisition platform. Within the scope of this work, a purchase of the data acquisition system was made in accordance with the system requirements discussed in the previous chapter. In addition, the equipment necessary to implement the new data acquisition system into the

test cell, and to integrate different measuring instruments, was purchased. The Dewesoft data acquisition system was chosen as the system implemented in this work and it is described thoroughly in the following subsection. The scope of the work in this thesis also included the supervision and reporting of the installation work related to the data acquisition system that was made on the test bench. Installation work included correct placement and mounting of the sensors, as well as electrical connections according to equipment manufacturers' instructions. This chapter discusses the work regarding installations, as well as describes in detail how the high sampling frequency measurement instruments were connected to the Dewesoft data acquisition system. Integration of low sampling frequency measurements into the Dewesoft data acquisition system via Modbus TCP/IP will be discussed in chapter 4.3.

4.2.1 Dewesoft data acquisition hardware

The hardware side of the Dewesoft data acquisition system implemented in this thesis consists of two 8-channel Dewesoft SIRIUS 8xSTG+ modules, the specification of which can be seen in Appendix 1. The modules are synchronized to align sampling between the channels. Every analog input (AI) channel has a ±50 V input range equipped with D-sub 9 connectors. They are galvanically isolated, which eliminates the formation of ground loops between channels. In addition to the AI channels, there are two counter channels per module as an option for digital counters. The maximum sampling rate per channel is 200 kHz and there are two 24-bit ADCs with built-in anti-aliasing filters for each channel. An anti-aliasing filter is a low-pass filter that blocks frequencies higher than those stated by the Nyquist theorem to prevent the aliasing effect. Even though the maximum sampling rate possible for the individual AI channels is 200 kHz, the ADCs oversample the signal at a high enough frequency in order to always satisfy the Nyquist criterion. After sampling, the data is filtered and downsampled to provide alias-free results (Dewesoft, 2022a). The topology of a single Dewesoft SIRIUS channel is shown in Figure 18.

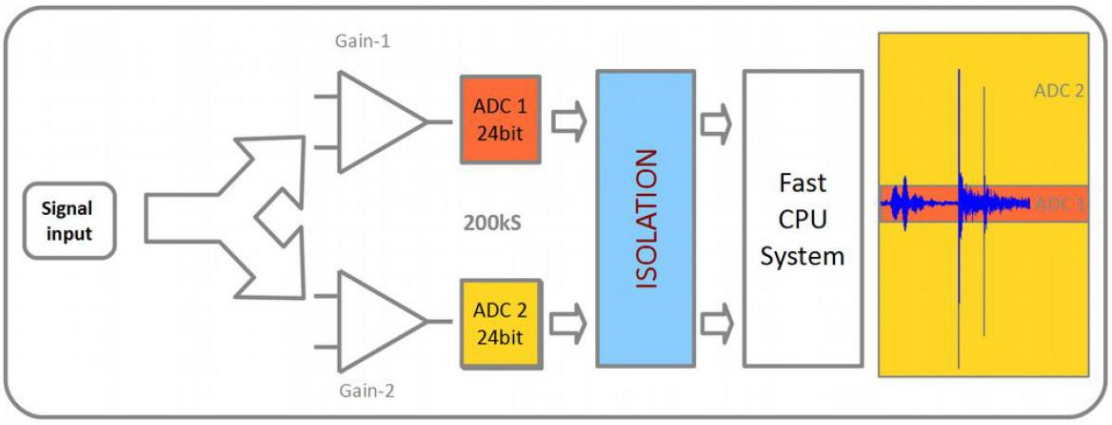

Figure 18. Topology of Dewesoft SIRIUS AI channel (Dewesoft, 2022a).

The Dewesoft SIRIUS utilizes trademarked Dual Core technology that enables measuring the signal using two ADCs with high and low gain simultaneously. The advantage of this is that the signal can be measured by using the full measurement range at all times without sacrificing the resolution (Smith, 2021). As illustrated in Figure 18, when the amplitude of the measured signal is too high for the ADC with a high gain amplifier (ADC 1), ADC with a lower gain amplifier (ADC 2) is used to prevent the signal from being out of range.

The counter channel of Dewesoft SIRIUS is able to count incoming pulse waves, such as in the TTL signal. A single counter channel has three digital inputs (DI) for different pulses and a ground connection. Additionally, 5 V or 12 V supply voltage and digital output are possible (Smith, 2021). The specifications of the counter channel are listed in Appendix 1. The counter channel of Dewesoft utilizes a trademarked technology called Super Counter. The architecture of the Super Counter is illustrated in Figure 19.

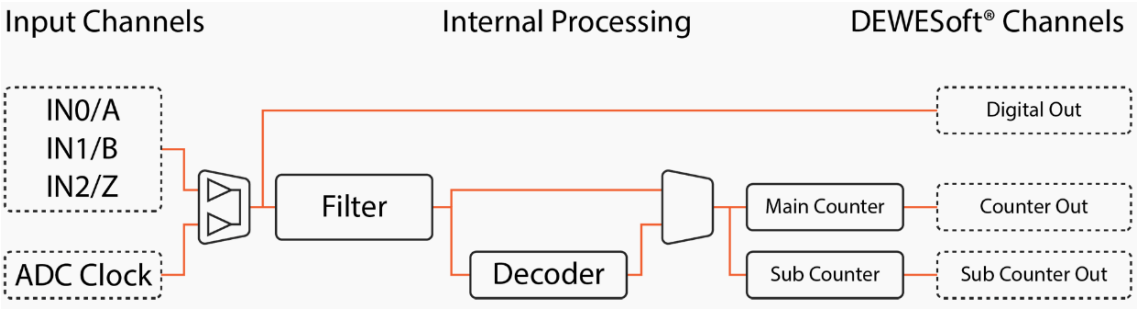

Figure 19. Dewesoft Super Counter architecture (Smith, 2021).

The Super Counter consists of two counters, both receiving the input signal. The main counter does the event counting, while the sub counter measures the exact time of the rising edge of a pulse signal. With this method, the counter can place event counts between pulse edges and interpolate sample points (Smith, 2021). The counter has a frequency of 102.4 MHz, which enables precise alignment of the pulse events in relation to the sampling of analog signals.

Dewesoft SIRIUS modules need to be connected to a computer equipped with DewesoftX software via separate USB 2.0 connections. Due to limitations in the maximum length of the USB 2.0 connection, the Black Box IC400A-R2 USB 2.0 extender is used. The selected USB 2.0 extender is equipped with 4 USB 2.0 ports and allows USB devices to be extended up to 100 meters over a twisted pair cable. Each port has a data transfer speed of up to 480 Mbps, which is the maximum for USB 2.0 (Compaq et al., 2000). These attributes make the selected USB 2.0 extender suitable to be used with Dewesoft SIRIUS hardware. The extender enables the Dewesoft SIRIUS modules in the test cell to be connected to the data acquisition computer located in the control room. Dewesoft SIRIUS modules are shown in Figure 20.

Figure 20. Dewesoft SIRIUS data acquisition hardware, installed in the VEBIC laboratory within the scope of the present work.

4.2.2 Installing the piezoresistive amplifiers

In the new RCCI test bench in VEBIC, every high-frequency piezoresistive transducer utilize TEDS. The amplifiers that are used for signal processing are all TEDS compatible, which enables automatic configuration. To configure the amplifier, an ethernet connection was established between the amplifier and a computer used in the configuration. When a TEDS device is connected to the amplifier, it automatically sets the correct parameters based on the characteristic values stored inside TEDS. This means that the amplifier is tuned for the correct range according to the transducer connected to it. Additionally, offset corrections can be applied if necessary. The output type can also be chosen via the configuration interface. For every amplifier, an output from 0 to 10 VDC was chosen so it can be connected to analog input (AI) channels of Dewesoft without any additional signal conversion. In order to ensure that the correct amplifier is always used with the transducer it was parametrized, transducers were assigned for a specific amplifier via configuration interface. This eliminates the possibility of connecting a wrong

transducer to the amplifier it was not parametrized to. Each amplifier is powered by 24 VDC power supply, which also supplies the power required by the transducer.

4.2.3 Electrical signal connections to data acquisition hardware

The two TTL signals from the encoder electronics are connected to the counter channel of the Dewesoft SIRIUS. Leads that carry the signals, as well as the common ground are connected to a 7-pin LEMO adapter, which is plugged to Dewesoft SIRIUS. The counter channel of Dewesoft provides the power supply of 12 VDC required by the encoder electronics. A high-frequency measurement chain is designed in a way that every continuous analog signal connected to AI channels of the Dewesoft hardware is a voltage signal. Additionally, they all are connected to AI channels using D-sub 9 to BNC (Bayonet Neill-Concelman) adapter.

In-cylinder pressure transducers are supplied with a 24 VDC and the output current signal is converted into a voltage signal using a resistor. When the current signal is flowing through a resistor, voltage generates across it according to Ohm's law. The output of 4–20 mA from the transducers is converted to 1–5 VDC signal using a 249 Ω resistor. The voltage signal from the in-cylinder pressure transducers is also connected to the AI card of the main Speedgoat for control applications. The disadvantage of using resistors is that they are a source of error due to their resistance being affected by temperature. Advantages are low cost and straightforward implementation. RCCI cylinder's intake and exhaust pressure transducers are connected to single-channel piezoresistive amplifiers and the voltage output is directly connected to the Dewesoft hardware. Additionally, current probes have voltage signal outputs that are connected to AI channels of the Dewesoft.

There are four signals related to EHVA's operation that are sampled with Dewesoft hardware. Valve position sensors of both gas exchange valves are supplied from a 24 VDC

power source and have a current output from 4 mA to 20 mA. Output signals are converted to 1–5 VDC using a 249 Ω resistor similarly to outputs from in-cylinder pressure transducers. These voltage signals are then connected in parallel with Dewesoft AI channels and AI channels of Speedgoat used to control EHVA. Gas exchange valve control signals from the AO channels of the Speedgoat range from 0 to 10 VDC. These signals are connected to both, AI channels of Dewesoft hardware and the signal converters.

Both fast emission analyzers are connected to their own computer via RS-485 serial connection. Analyzers have their specific control software that is used to operate them. Start-up, calibration, measurement, and shut-down procedures are all carried out via the software user interface. Measurement data itself is provided as 0–10 VDC analog output through the BNC outlet at the back of the analyzer. This output is directly proportional to the selected measurement range of the analyzer. Analog outputs from both analyzers are connected directly to AI channels of the Dewesoft via a BNC connector cable. In Table 4, every signal going to AI channels of the Dewesoft hardware is listed. Additionally, assigned channel names and output ranges of the signals are displayed. Measurement ranges of individual instruments are presented in Table 2.

Table 4. Electrical signal connections to Dewesoft AI channels.

Channel	Name	Description	Signal range
AI 1	Cyl1 pressure_ds	Cylinder 1 pressure	1–5 VDC
AI 2	Cyl2 pressure_ds	Cylinder 2 pressure	1–5 VDC
AI 3	Cyl3 pressure_ds	Cylinder 3 pressure	1–5 VDC
AI 4	Cyl4 pressure_ds	Cylinder 4 pressure	1–5 VDC
AI 5	Intake pressure_ds	Intake pressure	0–10 VDC
AI 6	Exhaust pressure_ds	Exhaust pressure	0–10 VDC
AI 7	InjectionCDC_ds	CDC injector currents	0–1 VDC
DI 8	Encoder_ds	Crank angle reference	TTL (0 or 5 V)
AI 9	InjectionPilot_ds	RCCI injector current	0–1 VDC
AI 10	IV position_ds	Intake valve position	1–5 VDC
AI 11	EV position_ds	Exhaust valve position	1–5 VDC
AI 12	IV control_ds	Intake valve control signal	0–10 VDC
AI 13	EV control_ds	Exhaust valve control signal	0–10 VDC
AI 14	FastNOx_ds	NOx concentration	0–10 VDC
AI 15	FastTHC_ds	THC concentration	0–10 VDC

4.3 Data acquisition system implementation

After installing and connecting the devices physically to the measurement system as discussed in chapter 4.2, the configuration of the channels and data acquisition software setup was conducted. In this chapter, the remaining issues regarding the integration of different measuring instruments to a common platform are discussed by explaining in detail about setting up the DewesoftX software. Settings configured for the signals directly connected to hardware and integration of low measurement frequency data from the test cell are further discussed. Post-processing of the measured quantities with DewesoftX is implemented in this section to provide a response to the third research question, concerning post-processing of the measurement data. In addition, an efficient way to store measurement and analysis data is discussed, which provides an answer to the fourth research question related to storing the data coming from the test bench.

4.3.1 Analog input channel configuration

Every channel used for measuring is configured according to the instrument connected to it. From the channel setup of DewesoftX software, channels are configured according to the measurement task. Figure 21 below shows the channel setup window, from where AI channel settings are configured.

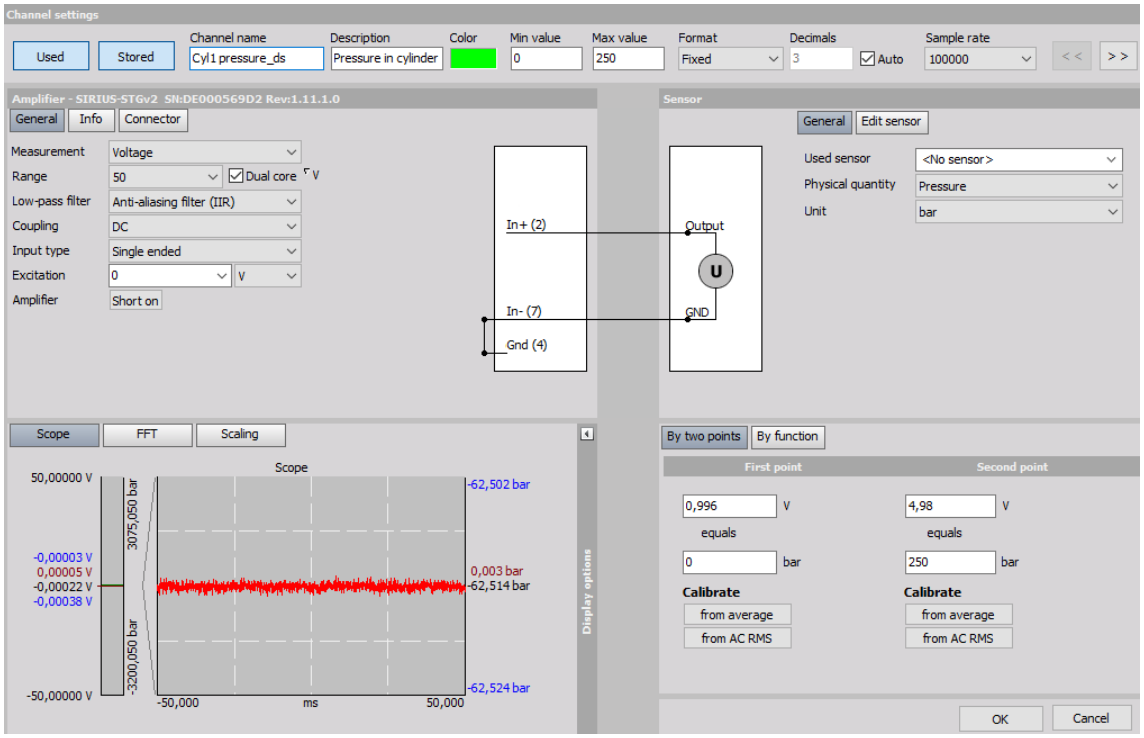

Figure 21. Channel setup window from DewesoftX.

A sampling rate of 100 kHz is selected for every AI channel. It is the closest sampling rate above 60 kHz that is possible to select. As discussed previously, assigned sampling rates for the AI channels already satisfy the Nyquist criterion due to automatic oversampling. Channels are given names and scaled so that the magnitude of measured voltage corresponds with the real value of the measured quantity. For scaling, the lowest and the highest points from the measurement range, as well as corresponding voltages are assigned. The relationship between the voltage and actual measurement value is assumed linear. The unit for the measured channel is selected according to the measured quantity and the range for each channel is selected as ±50 V. Dual Core is equipped on for each channel, which enables the use of the highest possible dynamic range. Additionally, a low-pass filter is assigned as an anti-aliasing filter in every channel. Inherent response delay from the fast emission analyzers needs to be considered during measurement. This is done by assigning a separate math channel to Dewesoft called the delay channel. It is meant to artificially delay or advance a signal by assigning a positive or negative time delay. In the case of fast emission analyzers, the assigned delay is negative because it

takes a few milliseconds for the analyzers to respond. The actual value of the time delay depends on the time between the opening of the exhaust valve and the response from the analyzer.

4.3.2 Counter channel configuration for encoder

To derive the correct speed and angular position of the crankshaft based on the TTL signal from the encoder, the counter channel must be configured accordingly. There are many predefined counter configurations in the software, but none of them was directly compatible with the Kistler 2614CK encoder. Because of this, a new counter type needed to be configured based on the used crank angle encoder. The selected sensor type working as a basis for the new encoder settings was a gear tooth with zero. Figure 22 shows the counter sensor editor window where new encoder settings were configured.

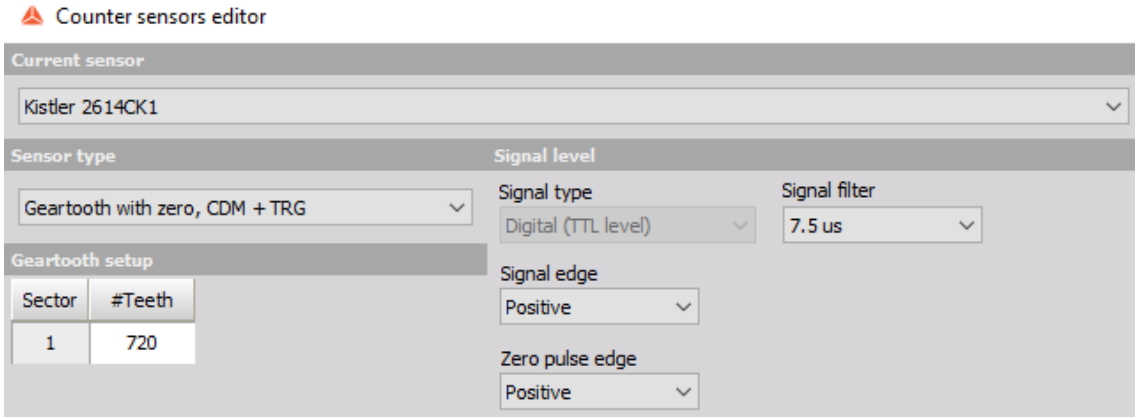

Figure 22. Counter sensor editor window in DewesoftX.

In the settings, the number of teeth was defined as 720. This corresponds to the number of pulses the encoder will output during one revolution. The rising edge of the zero pulse was selected to indicate a start of a new revolution, in accordance with the manual of Kistler 2614CK (Kistler, 2016). The signal filter is applied to prevent double counts and other disturbances. The time constant assigned to the filter determines the minimum time that signal must be present for the software to accept it as a valid signal. According

to Dewesoft (2022b), the selected value for the time constant must be lower than 10% of the minimum expected duration of an encoder pulse. Minimum pulse duration is achieved when the engine is running at its maximum speed of 1000 rpm. At this speed and 720 pulses per revolution, the frequency of the encoder signal, according to Equation 1, is 12 kHz. The time duration of a single pulse is an inverse of the frequency. From the calculated pulse duration, a time constant of less than 8.33 µs is required for the filter. Therefore, a value of 7.5 µs is selected.

4.3.3 CEA module configuration and parametrization

Combustion Engine Analysis (CEA) is a module for DewesoftX software that enables the measurement in the crank angle domain, as well as mathematics and statistics for combustion analysis (Dewesoft, 2022c). The configuration of the CEA module is divided into three sections in the software. The first section is the engine settings, where engine geometry and combustion-related parameters are defined, as well as additional channels for each cylinder are assigned. Assigning the channels to a specific cylinder enables the measurement of the parameters in crank angle domain and the alignment with respect to individual cylinder TDC. Figure 23 shows the parameters selected for the W4L20 RCCI test bench, as well as the additional channels assigned for each cylinder.

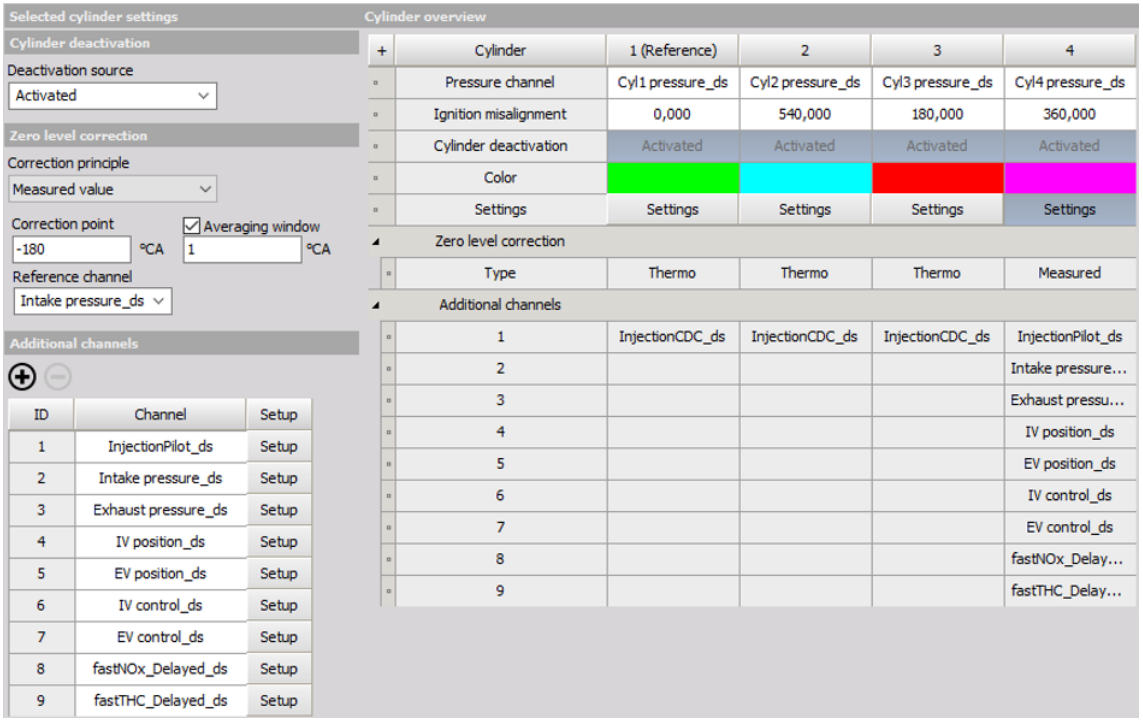

Figure 23. Selected parameters and additional channels assigned for the W4L20 RCCI test bench.

From the engine settings window, zero-level correction is also configured. The correction principle for the RCCI cylinder pressure is based on a measured value from the intake port pressure channel, which is selected as a reference channel. The selected correction point, at which the pressure curve is shifted according to the correction offset, is when the piston is at the BDC of the intake stroke. An averaging window of 1 CAD is selected, which determines the number of samples averaged in determining the value of pressure offset correction. In-cylinder pressure correction for other cylinders is selected as a thermodynamic correction principle.

Trigger levels for the start of injection (SOI) and end of injection (EOI), as well as the number of injections, are applied from the additional channel setup for injection signals. When the signal from the current probe exceeds the SOI trigger level or falls below the EOI trigger level, the corresponding crank angle position is recorded. Trigger levels of 0.3 V and 0.5 V are assigned for SOI and EOI respectively. Additionally, injection duration as milliseconds and crank angle degrees are calculated based on the triggering of SOI and

EOI events. The three cylinders operating in CDC all have the same current probe simultaneously measuring the injector currents. Therefore, it is necessary to distinguish which injection signal refers to which CDC cylinder's injection. To separate the signals from each other, the output of the current probe channels assigned for individual CDC cylinders is set to be active only for ±50 CAD relative to each cylinder's TDC during the compression stroke. Because injection happens during the assigned angle window, correct SOI and EOI events can be determined for separate cylinders.

After engine settings, the encoder settings are configured for the CEA module. The encoder type is selected as earlier configured Kistler 2614CK. The desired sample resolution is set to 0.1 CAD. The offset the between encoder trigger and TDC position is called trigger offset in the CEA module. An offset of 30 CAD is applied. It was determined manually by rotating the engine crankshaft and reading the position from the flywheel scale when the encoder triggers.

The result definition is made after applying the encoder settings. The CEA module includes basic real-time combustion analysis calculations and related statistics that can be enabled. Available results, as well as enabled calculations derived from the acquired in-cylinder pressure signals and crank angle are illustrated in Figure 24 below.

Toggle outputs

+	Group name	Current val.	Running avg.	Overall avg.	Cylinder avg.	Engine avg.	Setup
◢	Acquired signals						
▫	Pressure channels	Used	Unused	Unused			>
▫	Additional channels	Used	Unused	Unused			>
◢	Standard calculations						
▫	Maximum pressure	Used	Unused	Unused	Unused	Unused	Setup
▫	Compression curve	Unused	Unused	Unused			Setup
▫	Polytropic coefficient	Used	Unused	Unused	Unused	Unused	Setup
▫	Rise curve	Used	Unused	Unused			Setup
▫	Maximum rise	Used	Unused	Unused	Unused	Unused	Setup
▫	Mean effective pressure	Used	Unused	Unused	Unused	Unused	Setup
▫	Work	Used	Unused	Unused	Unused	Unused	
▫	Power	Used	Unused	Unused	Unused	Unused	
▫	Torque	Used	Unused	Unused	Unused	Unused	
▫	Thermodynamics 1	Unused	Unused	Unused	Unused	Unused	Setup
▫	Thermodynamics 2	Used	Unused	Unused	Unused		Setup
▫	Temperature	Unused	Unused	Unused			Setup
▫	Knocking (transient)	Unused	Unused	Unused	Unused	Unused	Setup
▫	Knocking	Unused				Unused	Setup

Figure 24. Result definition settings from DewesoftX showing the available and enabled basic calculations.

Every enabled calculation automatically creates corresponding channels to DewesoftX. Maximum pressure calculates the peak pressure and corresponding angle of each cycle. The polytropic coefficient returns the value as an output. The “rise curve” calculates the derivative of the pressure curve and the maximum rise returns the maximum rise value, as well as its position. Mean effective pressure calculates the $IMEP_g$, $IMEP_n$, and PMEP of each cycle. Work, power and torque calculations output a single value once per cycle. Thermodynamics 2 group name includes calculations of net heat release rate and cumulative heat release rate.

As stated in the literature review, most common combustion analysis systems ignore in-cylinder surface losses in the calculations. Accurate heat release rate calculation is re-

quired to be done separately, because the CEA module does not include gross heat release rate calculations. For calculating the gross heat release rate, the wall heat transfer rate is added to the result of the net heat release rate. Accurate gas-to-cylinder wall heat transfer real-time calculation model is not part of the thesis. However, it is part of another work task in the CPT project and the model is implemented to be a part of VEBIC's upgraded data post-processing routine.

4.3.4 Connecting the Modbus TCP/IP interface

As stated before, Modbus TCP/IP is the main communication interface in the W4L20 engine test cell. DewesoftX software is compatible with Modbus TCP/IP via separate plugin. The computer equipped with the software is connected to the Modbus TCP/IP network of the test cell in order to enable DewesoftX to poll data. Modbus plugin polls data from a channel of a Modbus device, when the IP address of the device and channel address are known. After polling the data, the value of the channel must be scaled according to the measurement device specification in order to align the raw data with the real measured value. Every channel sending measurement data from temperature data loggers, main Speedgoat, and PLC are added to DewesoftX through the Modbus plugin. Measurements include the data provided by both, instruments that were already installed in test bench and the ones that were added as a part of the modifications. The layout of how the channels are displayed in the DewesoftX can be seen in Appendix 2, where some of the channels that poll data from the test cell Modbus TCP/IP network are shown.

4.3.5 Monitoring interface

There are multiple options to setup the monitoring interface in DewesoftX software. The monitoring display can be configured to suit the preferences of the operator and requirements set by the measurement task. In general, cylinder pressures and results from real-time combustion analysis, such as IMEP and heat release calculations are important to

be monitored in the crank angle domain. In addition to CEA module calculations, every parameter sampled by Dewesoft AI channels can be monitored in the crank angle domain. A digital meter displaying the engine speed is also added to the monitoring interface. Low-frequency measurements logged to channels of DewesoftX via the Modbus plugin can also be displayed with digital meters, for example.

4.3.6 Data storing

DewesoftX software can record the raw high-frequency data sampled by the channels, data processed via the CEA module and other mathematical tools in the software, as well as the data polled from Modbus TCP/IP network. Data storing options in DewesoftX are configurable. The operator can choose the storing procedure to be manual or automatic. For the automatic storing option, different trigger conditions can be determined (Dewesoft, 2022d). Storage duration in DewesoftX can be selected as the amount of time or number of cycles. A thorough discussion regarding the selection of the storing option itself will not be covered in this thesis, because it depends on the purpose of the measurement and the preference of the operator.

The location for the created data files needs to be chosen before the measurement. Before starting the measurements, the data file is given a name that describes the measurement task. Dewesoft is configured to include a date and a running index number at the end of the file name in order to distinguish different files from each other. A common network location for the created data files was established as a part of this thesis. Files created with Dewesoft can be moved from a local storage to the network location manually or automatically by selecting it as a correct file path before starting the measurements. A disadvantage of automatically storing the data to the network location is its reliance on the internet connection. Figure 25 illustrates the designed folder structure and file naming scheme that enables a simple way of storing the data from different measurements.

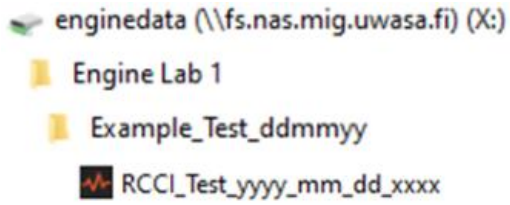

Figure 25. The designed folder structure for storing measurement data.

All the measurement data is saved to a network location. The data is always stored in a folder that corresponds to the test bench on which the measurements were made, as can be seen in Figure 25. Under the folder corresponding to the test bench, the operator creates a new folder with a name that describes the purpose of the test, as well as a date representing the time of the measurement. The data file created with the Dewesoft data acquisition system, containing the raw and processed data, is stored inside the created folder. As different measurements are made with the system, created data files are automatically assigned a date and a running index number at the end of the file name.

DewesoftX software can also be used to analyze and perform offline calculations on the raw measurement data. The advantage of using DewesoftX software is that it is free to use for analysis and does not require a separate license. The Dewesoft data file can be exported to multiple different formats, including text and CSV files. This allows the data to be used with another software. To export the acquired data, the user needs to select the format for the export file and data channels to be exported. There is also an option to perform statistical analysis while exporting the data. This means that for example averages and standard deviations of the variables can be calculated and exported. Appendix 3 includes a snippet of an example text-file that has been exported from Dewesoft data file. The file shows a part of the raw, crank angle-based measurement data from the EHVA unit test. It includes the names of the exported channels, units, and values at 0.1 CAD resolution. The EHVA unit test was made as a part of the system performance validation and will be discussed in chapter 5.2.

5 System consolidation and validation

5.1 System consolidation

One goal of the thesis was to design an integrated data acquisition system for Wärtsilä 4L20 engine test cell in VEBIC. The new W4L20 engine test cell data acquisition system is shown in Figure 26.

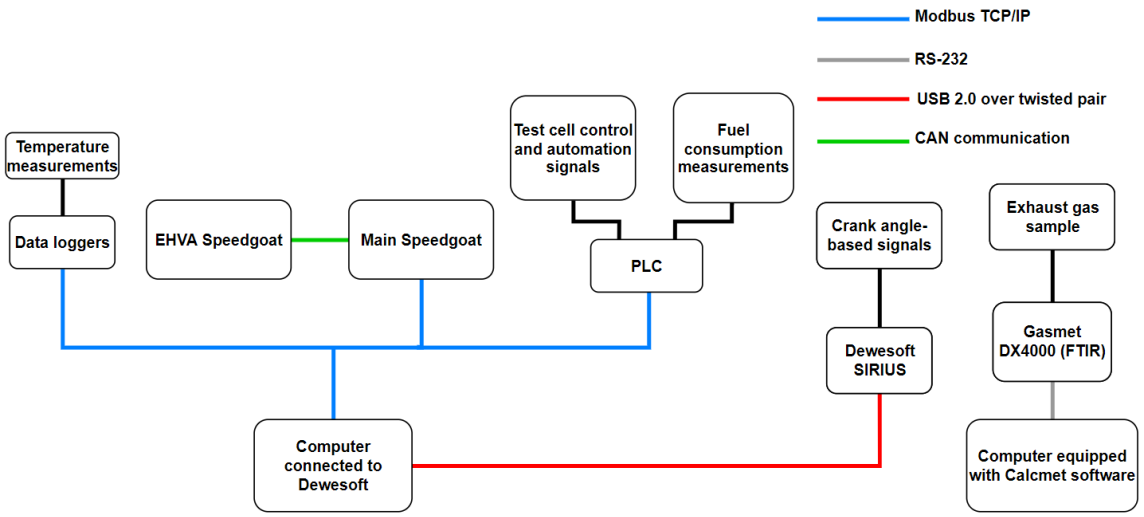

Figure 26. The layout of the W4L20 engine test cell data acquisition system designed in the thesis.

Compared to the previous data acquisition system in W4L20 engine test cell, the new system is more integrated. The previous system had separate systems collecting high-frequency and low-frequency data. The newly implemented data acquisition system measures high-frequency signals through its AI channels and collects low-frequency data from Modbus TCP/IP network, as illustrated in Figure 26. Therefore, a single Dewesoft data file contains both, high and low-frequency data. In the thesis, integration of the FTIR analyzer output was not implemented.

5.2 System performance validation

5.2.1 High sampling frequency measurement system evaluation

Selected new instruments are of high quality. Therefore, they can be expected to function well for a long time as long as proper maintenance and calibration is done according to manufacturer's requirements. Systematic measurement uncertainty, according to Equation 15, was calculated for high-frequency analog signals acquired through Dewesoft. Error calculation of injector current signals was left out, as they are only used to trigger SOI and EOI events. Therefore, measurement accuracy is not crucial. Results of the uncertainty calculation are shown in Appendix 4. Errors for every individual part of the measurement chain were obtained from data sheets provided by device manufacturers. Conversion errors were included in cases where an external amplifier or a resistor is used to convert the signal into voltage. Errors resulting from signal transmission were assumed low enough to be disregarded. Cables that were used to transmit analog signals to Dewesoft were shielded. Because these signals are transmitted as voltage signals, distances were designed to be as short as possible. Additionally, it was avoided to install cables near places where significant electrical interference is possible.

5.2.2 The EHVA unit test conditions

At the time of writing this thesis, all modifications to enable RCCI operation in the W4L20 test bench are not finished. This poses limitations in validating the whole data acquisition system while simultaneously operating the engine in RCCI mode. Therefore, in order to validate the performance of the implemented data acquisition system, unit test of the EHVA was performed instead of the whole engine. During the EHVA unit test, only the valves of the RCCI cylinder were actuated through the Speedgoat. Engine crankshaft was locked to BDC position to avoid collision with the valves while operating the EHVA. In the test, crank angle reference signal was provided by a separate pulse wave signal generator.

The signal generator mimics the signal coming from the actual gear tooth sensor of the engine, which is a conventional 120-1 sensor, and is connected to the Dewesoft data acquisition system and Speedgoat control system. In the DewesoftX software, there is an in-built configuration for a conventional 120-1 gear tooth sensor, which was used during the unit testing of the EHVA system. Other signals acquired with Dewesoft during the EHVA unit test were valve position signals from the sensors and control signals from the EHVA Speedgoat's AO card. The connections have already been discussed. Except for the counter settings, configuration of the data acquisition system for the EHVA unit test do not differentiate from the settings already made for the whole test bench.

During the EHVA unit test, engine speed parameter was changed by changing the frequency output from the signal generator. The EHVA was operated through the Speedgoat and the measurements were done with the Dewesoft system. During the test, Dewesoft data acquisition system was able to record the high-speed signals related to EHVA operation.

5.2.3 Results of the EHVA unit test

Appendix 5 shows the analog signal curves acquired by the data acquisition system during the test in time domain for a period of 1 second. One discovery during the EHVA unit test was that even though the valves are closed, the value of the valve position does not reach zero mainly because the sensors are actually measuring the movement of the valve actuators. This problem was solved by creating a math channel in DewesoftX to correct the valve position curves. Correction for every cycle was made by shifting the valve position curves in the crank angle plane according to the offset value. The offset value for each individual cycle was determined as the value of the valve position signal at the TDC, when both valves are supposed to be fully closed. In Figure 27 there are corrected intake valve and exhaust valve position curves, as well as the corresponding control signal curves measured by the data acquisition system with respect to crank angle at 520 rpm.

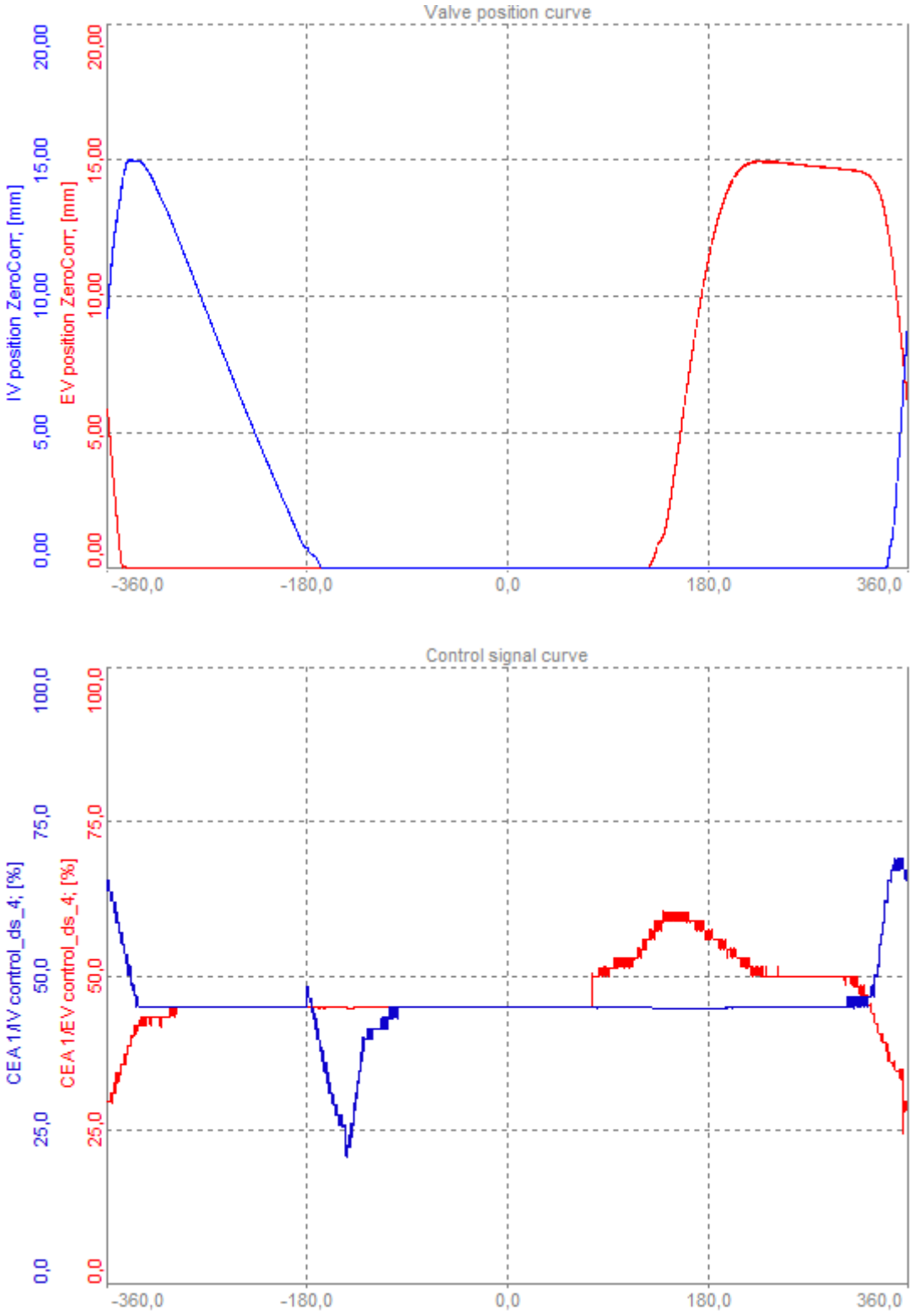

Figure 27. Position and control signal curves of intake (blue) and exhaust (red) valves with respect to crank angle.

The maximum lift parameter was assigned as 15 millimeters for the intake and exhaust valves. It can be seen from the measured position curves that the maximum position is at 15 millimeters for both valves. In addition, both position curves reach zero at TDC. Therefore, the measured position curves are according to these assigned position parameters and the zero correction of the curves function properly. As can be seen from the control signal curve, the Speedgoat sends a signal to open the exhaust valves at approximately 80 CAD after TDC, and the valve starts to open at 130 CAD after TDC. In the case of the intake valves, the control signal is sent at approximately 300 CAD after TDC and the valves start to open at 340 CAD after TDC. The time difference between sending the signal and the valve opening occurs due to the response time of the hydraulic valves and the mechanical inertia associated with the system. No correction is needed for the control signals, because the measurement is taken directly from the AO card of the EHVA Speedgoat. The values of the valve positions are at 0.1 resolution and there is no aliasing in the curves. Therefore, the sampling rate is sufficient for the channels. The results in the EHVA unit test were meant only to verify that the system works properly. In the future, operation of the system will be optimized.

Before the measurements, a new folder designated for the EHVA unit test was created in the network location and it was selected as the destination folder for the data files. Therefore, data files created during the measurements were automatically stored to the correct folder in the network location. From the EHVA unit test, it can be concluded that the data acquisition system implemented in this thesis enables the monitoring and storage of the measurement data with respect to crank angle.

5.3 Prospects for system expansion

The data acquisition system designed and implemented in this thesis has opportunities to expand and adapt to many needs that potentially arise in the VEBIC laboratory of the university of Vaasa. The number of channels in the Dewesoft hardware can be expanded by purchasing additional modules. In theory, there is no upper limit for the number of

possible high-speed AI channels. Dewesoft SIRIUS is compatible with practically any basic measurement device, when a proper connection adapter is purchased. For example, in addition to measurements introduced in this thesis, Dewesoft SIRIUS is capable of measuring vibration, torsion and stress measurements. Cameras can also be integrated with the Dewesoft system, if there arises a requirement for optical measurements. All input types that are compatible with AI channels of Dewesoft SIRIUS modules are listed in the specification of Appendix 1. In addition, there are many tools in DewesoftX for analyzing different types of data and the capabilities can be extended via user-defined C++ code.

In this thesis, the possibility to integrate the FTIR analyzer was also explored. It is possible to have DewesoftX software poll data from the channels of Calcmet software used for FTIR analysis. Integration would require Modbus RTU to Modbus TCP/IP gateway between the computers operating the FTIR analyzer and DewesoftX respectively. The implementation of the integration was left out from the scope of this thesis.

One example of the future need for expansion is an upcoming project called Silent Engine which aims to seek methods to reduce noise and vibration resulting from engines. In the project (Silent Engine, 2022), accelerometers and microphones are planned to be employed in order to measure vibrations, as well as sound power in several locations. These measurements are already possible with the data acquisition system implemented in this thesis. Accelerometers and microphones can be directly connected to the AI channels of Dewesoft SIRIUS hardware when they are connected through a proper signal amplifier. Different amplifiers meant for accelerometers and microphones can relatively easily be found on the markets. For example, Dewesoft provides adapters that allow the connection of accelerometers and microphones to the SIRIUS hardware. Analysis of vibration and sound are also possible with the Dewesoft data acquisition system. From the data obtained through accelerometers, displacement and velocity can be automatically calculated in the DewesoftX software. Additionally, DewesoftX software can perform FFT and modal analysis for vibration measurements. In the case of acoustic measurements,

there are tools in the software that enables power, intensity, and quality analysis to be made for sound measurements (Dewesoft, 2022d).

6 Conclusions

The goal of the thesis was to design and implement a data acquisition system for large-bore state-of-the-art engine test bench. Reaching the goal was enabled by meeting the objective of this research, which was to discover the requirements for the new data acquisition system in order to provide more fluent low-temperature combustion research for the RCCI engine. Within the scope of this thesis, a data acquisition system for a test bench featuring large-bore RCCI engine with state-of-the-art instrumentation and a high level of integration was designed and built. Aside to general goal and objective, this thesis aimed to provide answers to four specific research questions. The answers to these research questions are provided here as specific conclusions.

Concerning research question 1 – measurement system requirements to enable LTC research on a multi-cylinder engine. It is important for an engine test cell data acquisition system to be able to simultaneously make and record slow measurements, as well as fast measurements that are in reference to crank angle. In addition, the system needs to be able to perform extensive post-processing of the directly measured values in real-time for combustion monitoring purposes. It can be concluded that unique feature of a system dedicated to LTC research is the emphasis on accurately determining the intake valve closing conditions and the burn rate. To enable a more accurate determination of heat release rate, crank angle-based intake and exhaust pressure need to be measured. This provides a more accurate zero-level correction and estimation of the flow rates in and out of the cylinder. By determining accurate flow rates, more precise estimation of in-cylinder gas composition and the polytropic coefficient is possible. The fully variable valve train applied in a unique implementation of the discussed RCCI engine further reinforces the need for this accuracy, while introducing the additional requirements for fast response emission analysis associated with precise valve position measurement.

Concerning research question 2 – integration of different measuring instruments into a common data acquisition platform, which involves a large amount of measurement

signals. Conclusion is that for a data acquisition system to be able to include multiple different measuring instruments, it is required to be able to read different types of device inputs directly or through an external signal conversion. The input cards and signal converters need to be selected according to the type of the measured signal, as well as the required sampling frequency that satisfies the Nyquist criterion. It should be noted that additional signal conversion steps in the system introduce more overall errors. In addition, the system should be able to read data through necessary communication protocols that the devices are compatible with. To substantiate this conclusion, the work successfully integrated over 40 instruments with several different signal type and sample rate combinations into a common data acquisition platform. Note that the pre-existing system already had several instruments installed and a governing Modbus TCP/IP communication protocol. It was a requirement for the implemented system to be able to poll data from the already existing system.

Concerning research question 3 – efficient post-processing of the measured quantities that enables insight into the in-cylinder phenomena. Different methodologies related to the in-cylinder pressure data post-processing, combustion analysis, as well as statistical tools to validate measurement repeatability and cyclic variability of combustion were discussed in detail in the thesis. The conclusion for the research question is that the real-time post-processing of the measured quantities, such as zero-level correction and the heat release calculations, could be implemented with the tools provided by the purchased combustion analysis module. The real-time capabilities of the system are the key feature that enables efficient post-processing and give immediate access to information regarding the in-cylinder phenomena. Important aspect of the implemented zero-level correction is that it is based on the measured crank angle-based intake port pressure, which enables accurate correction of the in-cylinder pressure curve. This, together with analyzing the in-cylinder flows, enables a deep understanding of the in-cylinder combustion process. Statistical analysis of the variables was carried out with the mathematical tools of the system.

Concerning research question 4 – efficient storing of large amount of measurement data from an engine test bench. It can be concluded that the extensive data storage provided by a network storage location coupled with storing functionalities of the system implemented in this thesis provide an efficient way of storing measurement data. The designed folder structure on the other hand enables a consistent method of storing data from multiple measurements. Engine test data storage requires an extensive capacity, as well as consistent folder structure to ease the data management. Variable naming is also crucial when there are many different measured variables that need to be stored and distinguished from one another.

7 Summary and outlook

There are multiple improvements that the measurement system designed and implemented in this thesis provides compared to the system previously used in the W4L20 test cell at VEBIC. The upgraded data acquisition system is more integrated than the previous one. Previously, the data from measurements with high sample rate and low sample rate were recorded with different systems running on different computers. This resulted in the data being distributed into two different locations which made the data management very challenging. After the implementation of the new system carried out in this thesis, the level of measurement data integration has improved significantly. The data acquisition system of the W4L20 test cell is now capable of making high-speed and low-speed measurements simultaneously, as well as storing them to the same data file. In addition, the number of channels capable of high-speed measurements was increased significantly from 8 to 16, resulting to more possibilities in conducting crank angle-based measurements. In addition, the capabilities of the real-time post-processing increased due to more integrated data acquisition and an increased number of high-speed channels. Compared to the previous system, the upgraded system offers integration of a wider range of different types of inputs for measurements with high sample rate without the need for significant changes to the system. In addition, it is possible for the new measurement system to expand in order to meet the requirements that may arise in the future.

Although it was not possible to validate the whole measurement system, the EHVA unit test provided results that the system was capable to measure quantities in reference to crank angle. It should be noted that the whole system will be validated when it is possible to run the engine in the future. Based on the validation of the whole system, adjustments will be performed on the system if necessary. When the capabilities of the data acquisition system designed and implemented in the thesis are considered, it can be concluded that it is suitable for performing measurements on the W4L20 RCCI engine test bench.

References

Asad, U., Kumar, R., Han X. & Zheng, M. (2011). Precise instrumentation of a diesel single-cylinder research engine. *Measurement, 44*, 1261–1278. https://doi.org/10.1016/j.measurement.2011.03.028

Atkins, R. (2009). *An Introduction to Engine Testing and Development*. SAE International.

Baškovič, U., Vihar, R., Oprešnik, S., Seljak, T. & Katrašnik, T. (2022). RCCI combustion with renewable fuel mix – Tailoring operating parameters to minimize exhaust emissions. *Fuel, 311*. https://doi.org/10.1016/j.fuel.2021.122590

Cambustion. (2008). *CLD500 – Fast NOx Measurement System User Manual (version 2.2)*

Cambustion. (2004). *HFR500 – Fast Response FID Hydrocarbon Measurement System User Manual (version 2.8)*

Chen, S., Meng, Q., Jia, P. & Kuang, H. (2021). An operational-mode-based method for estimating ship emissions in port waters. *Transportation Research Part D: Transport and Environment, 101*. https://doi.org/10.1016/j.trd.2021.103080

Clean Propulsion Technologies. (2021). Project website. Accessed 05-09-2022 in https://cleanpropulsion.org/

Compaq, Hewlett-Packard, Intel, Lucent, Microsoft, NEC & Philips. (2000). Universal Serial Bus Specification Revision 2.0. Received 07-03-2022 from https://www.usb.org/document-library/usb-20-specification

Dewesoft. (2022a). *Dewesoft SIRIUS – Technical reference manual*. Received 26-05-2022 from https://d36j349d8rqm96.cloudfront.net/3/6/Dewesoft-SIRIUS-Manual-EN.pdf

Dewesoft. (2022b). *Measure Angle and Frequency With Digital Counters*. Received 26-05-2022 from https://training.dewesoft.com/online/course/digital-counters

Dewesoft. (2022c). *Combustion Engine Analysis – CEA – Software user manual*. Received 26-05-2022 from https://d36j349d8rqm96.cloudfront.net/3/116/Combustion-Engine-Analysis-CEA-Manual-EN.pdf

Dewesoft. (2022d). *DewesoftX User Manual – English*. Received 26-05-2022 from https://d36j349d8rqm96.cloudfront.net/3/8/DewesoftX3_User_Manual.pdf

Duan, X., Lai, M.-C., Jansons, M., Guo, G. & Liu, J. (2021). A review of controlling strategies of the ignition timing and combustion phase in homogeneous charge compression ignition (HCCI) engine. *Fuel, 285*. https://doi.org/10.1016/j.fuel.2020.119142

European Union. (2009). REGULATION (EC) No 595/2009 OF THE EUROPEAN PARLIAMENT AND OF THE COUNCIL of 18 June 2009 on type-approval of motor vehicles and engines with respect to emissions from heavy duty vehicles (Euro VI) and on access to vehicle repair and maintenance information and amending Regulation (EC) No 715/2007 and Directive 2007/46/EC and repealing Directives 80/1269/EEC, 2005/55/EC and 2005/78/EC. https://eur-lex.europa.eu/legal-content/EN/TXT/?uri=CELEX%3A32009R0595&qid=1664803993900

Ferguson, C. & Kirkpatrick, A. (2015) *Internal Combustion Engines: Applied Thermosciences* (2nd edition). John Wiley & Sons, Inc.

Fluke. (2017). *80i-110s AC/DC Current Probe – Instructions*. Received 29-04-2022 from https://dam-assets.fluke.com/s3fs-public/80i110s_is-eng0100.pdf?XFS2MXiqNYqJX6B5U47dUNjZ575.U_sv

Gasmet. (2020). FTIR Gas Analysis. White paper. Received 09-02-2022 from https://www.gasmet.com/whats-new/white-papers/

Hautala, S., Mikulski, M., Söderäng, E., Storm, X. & Niemi, S. (2022). Toward a digital twin of a mid-speed marine engine: From detailed 1D engine model to real-time implementation on a target platform. *International Journal of Engine Research*. https://doi.org/10.1177/14680874221106168

Heywood, J. (2018). *Internal Combustion Engine Fundamentals* (2nd edition). McGraw-Hill Education.

Indrajuana, A., Bekdemir, C., Luo, Xi. & Willems, F. (2016). Robust Multivariable Feedback Control of Natural Gas-Diesel RCCI Combustion. *IFAC-PapersOnLine, 49-11.* https://doi.org/10.1016/j.ifacol.2016.08.033

Isermann, R. (2014). *Engine Modeling and Control – Modeling and Electronic Management of Internal Combustion Engines*. Springer. https://doi:10.1007/978-3-642-39934-3

Jiang, S., Smith, M., Kitchen, J. & Ogawa, A. (2009). Development of an Engine-in-the-loop Vehicle Simulation System in Engine Dynamometer Test Cell. *SAE Technical Paper*. https://doi.org/10.4271/2009-01-1039

Kaprzyk, P., Hunicz, J., Rybak, A., Geca, M. & Mikulski, M. (2020). Excess Air Ratio Management in a Diesel Engine with Exhaust Backpressure Compensation. *Sensors, 20*. https://doi.org/10.3390/s20226701

Kistler. (2016). *Crank angle encoder set - Precise angle signals from 0 ... 12 000 1/min*. Received 23-04-2022 from https://www.kistler.com/files/document/003-043e.pdf?callee=frontend

Kistler. (2018). *Cylinder pressure sensor for on-line combustion control*. Received 23-04-2022 from https://www.kistler.com/files/document/003-043e.pdf?callee=frontend

Kistler. (2020). *Test & measurement pressure - Measurement equipment for demanding T&M applications*. Received 08-02-2022 from https://www.kistler.com/files/download/960-695e.pdf

Klein, S., Savelsberg, R., Xia, F., Guse, D., Andert, J., Blochwitz, T., Bellanger, C., Walter, S., Beringer, S., Jochheim, J. & Amringer, N. (2017). Engine in the Loop: Closed Loop Test Bench Control with Real-Time Simulation. *SAE International Journal of Commercial Vehicles, 10*(1), 95–105. https://doi.org/10.4271/2017-01-0219

Kline, S. & McClintock, F. (1953). Describing Uncertainties in Single Sample Experiments, *Mech. Eng, 75*, 3–8.

Kokjohn, S., Hanson, R., Splitter, D. & Reitz, R. (2011). Fuel reactivity controlled compression ignition (RCCI): a pathway to controlled high-efficiency clean combustion. *International Journal of Engine Research, 12*(3). https://doi.org/10.1177/1468087411401548

Krishnamoorthi, M., Malayalamurthi, R., He, Z. & Kandasamy, S. (2019). A review on low temperature combustion engines: Performance, combustion and emission characteristics. *Renewable and Sustainable Energy Reviews, 116*. https://doi.org/10.1016/j.rser.2019.109404

Lee, Y. & Min, K. (2019). Estimation of the polytropic index for in-cylinder pressure prediction in engines. *Applied Thermal Engineering, 158*. https://doi.org/10.1016/j.applthermaleng.2019.04.113

Li, J., Yang, W. & Zhou, D. (2017). Review on the management of RCCI engines. *Renewable and Sustainable Energy Reviews, 69,* 65–79. https://doi.org/10.1016/j.rser.2016.11.159

Martyr, A. & Plint, M. (2012). *Engine Testing: The Design, Building, Modification and Use of Powertrain Test Facilities* (4th edition). Butterworth-Heinmann. https://doi.org/ 10.1016/B978-0-08-096949-7.00001-7

Masson-Delmotte, V., Zhai, P., Pörtner H.-O., Roberts D., Skea J., Shukla P.R., Pirani A., Moufouma-Okia, W., Péan C., Pidcock R., Connors S., Matthews J.B.R., Chen Y., Zhou X., Gomis M.I., Lonnoy E., Maycock T., Tignor M., & Waterfield, T. (2018). *An IPCC Special Report on the impacts of global warming of 1.5°C above pre-industrial levels and related global greenhouse gas emission pathways, in the context of strengthening the global response to the threat of climate change, sustainable development,* IPCC. Received 13-01-2022 from https://www.ipcc.ch/site/assets/uploads/sites/2/2019/06/SR15_Full_Report_High_Res.pdf

Measurement Computing. (2012). *Data acquisition handbook: a reference for DAQ and analog & digital signal conditioning* (3rd edition). Received 24-02-2022 from https://www.mccdaq.com/pdfs/anpdf/data-acquisition-handbook.pdf

Merker, G., Schwartz, C. & Teichmann, R. (2012). *Combustion Engines Development: Mixture Formation, Combustion, Emissions and Simulation*. Springer. https://doi.org/10.1007/978-3-642-14094-5

Merts, M., Derafshzan, S., Hyvönen, J., Richter, M., Lungren, M. & Verhelst, S. (2021). An optical investigation of dual fuel and RCCI pilot ignition in a medium speed engine. *Fuel Communications, 9*. https://doi.org/10.1016/j.jfueco.2021.100037

Mestemaker, B., Van Biert, L. & Visser, K. (2020). The maritime energy transition from a shipbuilder's perspective. *International Naval Engineering Conference*. https://doi:10.24868/issn.2515-818X.2020.027

Mikulski, M., Duda, K. & Wierzbicki, S. (2016). Performance and emissions of a CRDI diesel engine fuelled with swine lard methyl esters–diesel mixture. *Fuel, 164*, 206–219. https://doi.org/10.1016/j.fuel.2015.09.083

Mikulski, M. (2021). Finland looks to develop dual-fuel RCCI engine tech. *Motor Ship, 102*(1189), 18-19.

Modbus Organization. (2006). MODBUS Messaging on TCP/IP Implementation Guide V1.0b. Received 16-03-2022 from https://www.modbus.org/docs/Modbus_Messaging_Implementation_Guide_V1_0b.pdf

Morris, A. & Langari, R. (2012). *Measurement and instrumentation: theory and application* (1st edition). Elsevier Inc.

Nakamura, H. & Adachi, M. (2013). *Engine Emissions Measurement Handbook* (1st edition). SAE International and Horiba Ltd.

National Instruments. (2021). Measuring Position and Displacement with LVDTs. Received 11-02-2022 from https://www.ni.com/fi-fi/innovations/white-papers/06/measuring-position-and-displacement-with-lvdts.html

Osman, A. & Massoud, M. (2013). Setting up a data acquisition system for spark engines. *Annual International Interdisciplinary Conference*.

Panda, K. & Ramesh, A. (2022). Parametric investigations to establish the potential of methanol based RCCI engine and comparison with the conventional dual fuel mode. *Fuel, 308*. https://doi.org/10.1016/j.fuel.2021.122025

Paykani, A., Kakaee, A.-H., Rahnama, P. & Reitz, R. (2016). Progress and recent trends in reactivity-controlled compression ignition engines. *International J of Engine Research, 17*(5)*, 481–524.* https://doi.org/ 10.1177/1468087415593013

Rogers, D. (2010). *Engine Combustion: Pressure Measurement and Analysis*. SAE International. https://doi.org/ 10.4271/R-388

Silent Engine. (2022). Project website. Accessed 20-09-2022 from https://www.uwasa.fi/en/research/projects/silent-engine

Shim, E., Park, H. & Bae, C. (2020). Comparisons of advanced combustion technologies (HCCI, PCCI, and dual-fuel PCCI) on engine performance and emission characteristics in a heavy-duty diesel engine. *Fuel, 262*. https://doi.org/10.1016/j.fuel.2019.116436

Smith, C. (2009). *Basic Process Measurements*. John Wiley & Sons, Inc.

Smith, G. (2021). *Dewesoft Data Acquisition Technology Explained*. Dewesoft. https://dewesoft.com/daq/dewesoft-data-acquisition-technology-explained#dualcoreadc

Sogbesan, O. (2016). *Strategies for Reducing Hydrocarbon Emissions in Diesel Low Temperature Combustion.* [Doctoral dissertation, Loughborough University]. Loughborough's Research Repository.

SST Sensing Ltd. (2017). O_2 Sensors – Zirconium Dioxide (ZrO_2) Oxygen Sensor Operating Principle Guide. Received 07-03-2022 from https://sstsensing.com/wp-content/uploads/2016/05/AN-0043_rev5_Zirconia-Sensor-Operating-Principle-and-Construction-Guide.pdf

Söderäng, E., Hautala, S., Mikulski, M., Storm, X. & Niemi, S. (2022). Development of a digital twin for real-time simulation of a combustion engine-based power plant with battery storage and grid coupling. *Energy Conversion and Management, 266*. https://doi.org/10.1016/j.enconman.2022.115793

Teter, J., Tattini, J. & Petropoulos, A. (2020). Tracking Transport 2020. *IEA*. Retrieved 13-01-2022 from https://www.iea.org/reports/tracking-transport-2020

United Nations. 2015. Paris Agreement. Received 13-01-2022 from https://unfccc.int/sites/default/files/english_paris_agreement.pdf

Clean Propulsion Technologies. (2021). WP3 Novel combustion and advanced aftertreatment. Retrieved 21-08-2022 from https://cleanpropulsion.org/project/wp3

Wang, Z., Pan, X., Zhang, W., Zhao, Y., Li, H. and Liu, P. (2020). The Development Trend of Internal Combustion Engine. *International Conference on Electrical Automation and Mechanical Engineering*. https://doi:10.1088/1742-6596/1626/1/012139

Wei, L. & Geng, P. (2015). A review on natural gas/diesel dual fuel combustion, emissions and performance. *Fuel Processing Technology, 142, 264–278*. https://doi.org/10.1016/j.fuproc.2015.09.018

Willems, R., Willems., F., Deen, N. & Somers, B. (2021). Heat release rate shaping for optimal gross indicated efficiency in a heavy-duty RCCI engine fueled with E85 and diesel. Fuel, 288. https://doi.org/10.1016/j.fuel.2020.119656

Williams, M. & Minjares, R. (2016). A technical summary of Euro 6/VI vehicle emission standards. The International Council on Clean Transportation. Received 16-03-2022 from https://theicct.org/wp-content/uploads/2021/06/ICCT_Euro6-VI_briefing_june2016.pdf

Zhang, D., Huichao, X., Shimin, H. & Xiangyi, W. (2014). Design of the Parameters Acquisition and Analysis System on Marine Diesel Engine. *International Conference on Mechatronics and Automation*. https://doi.org/ 10.1109/ICMA.2014.6886013

Zhang, D. & Liu, Y. & Gao, J. (2018). Development of Operating Parameters Acquisition System on Marine Diesel Engine. *International Conference on Mechatronics and Automation*. https://doi.org/10.1109/ICMA.2018.8484732

Appendices

Appendix 1. Specification of Dewesoft SIRIUS STG module.

5.14.1. STGv2: Specifications

Inputs				
Input types	Voltage Full/Half/Quarter bridge strain (120 Ω and 350 Ω) Potentiometer, RTD, Resistance Current (ext. Shunt)			
ADC Type	24-bit delta-sigma dual core with anti-aliasing filter			
Sampling Rate	Simultaneous 200 kS/sec			
Dual Core Ranges (Low)	**±50 V (±2.5 V)**	**±10 V (±500 mV)**	**±1 V (±50 mV)**	**±100 mV (±5 mV)**
Gain accuracy	±0.05 % of reading			
Offset accuracy (Dual Core)	±20 (10) mV	±2 (1) mV	±0.2 (0.2) mV	±0.1 (0.1) mV
Offset Accuracy after Balance Amplifier	±1 mV	±0.1 mV	±0.02 mV	±0.01 mV
Typ. Dynamic Range @ 10 kS (Dual Core)	-137 dB (-147 dB)	-137 dB (-152 dB)	-137 dB (-147 dB)	-135 dB (-137 dB)
Typ. Noise floor @ 10kS (Dual Core)	-108 dB (-118 dB)	-107 dB (-125 dB)	-107 dB (-113 dB)	-100 dB (-100 dB)
Typ. CMR @ DC...50 Hz / 400 Hz / 1 kHz	56 / 56 / 56 dB	88 / 86 / 84 dB	97 / 96 / 95 dB	115 / 112 / 102 dB
Gain Drift Typical	10 PPM/K, max. 40 PPM/K			
Offset Drift Typical	0.3 µV/K + 2 ppm of range/K, max 0.8 µV/K + 10 ppm of range/K			
Gain Linearity	<0.02 %			
Inter Channel Phase-mismatch	0.02° * fin [kHz] + 0.1° (@ 200 kS/sec)			
Channel Crosstalk	-120 dB @ 10 kHz			
Input Coupling	DC, AC 1 Hz (3 Hz, 10 Hz per SW)			
Input Impedance	1 MΩ between IN+ and IN- for 50 V Range; all other Ranges > 1 GΩ			
Max. Common Mode Voltage	Isolated version: ±500 V Differential version: 50 V Range: ±60 V; all other Ranges: ±12 V			
Overvoltage Protection	50 V Range: 300 V; all other Ranges: 50 V (200 V peak for 10 msec)			
Excitation Voltage				
Excitation Voltage	Free programmable (16-bit DAC)			
Predefined levels	0, 1, 2.5, 5, 10, 15 and 20 VDC			
Accuracy	±0.05 % ±2 mV			
Drift	±10 ppm/K ±100 µV/K			
Load stability	0 % to 100 % load <0.01 %			
Noise @ 10V / 350 Ω	<150 µVrms @ 10 kS			
Line regulation over 20 Ω of change	<0.005 % @ 120 Ω load			

Sense Impedance to Exc / to GND	100 kΩ / >100 MΩ			
Current limit	100 mA (max. 800 mW)			
Protection	Continuous short to ground			
Excitation Current	**STGv2**		**STGv3**	
Excitation Current	Free programmable (16-bit DAC)			
Predefined levels	0.1, 1, 2, 5, 10, 20 and 60 mA DC			
Ranges	0.1 - 10 mA	10 - 60 mA	0.01 - 1 mA	1 - 60 mA
Accuracy	0.1 % ±2 µA	0.5 % ±50 µA	preview 0.02 % ±2 µA	preview 0.25 % ±20 µA
Drift	15 ppm/K	100 ppm/K	preview 15 ppm/K	preview 100 ppm/K
Compliance voltage	20 Volt, max. 500 mW			
Output Impedance	>1 MΩ			
Bridge Connection Types				
Bridge types	Full / Half / Quarter bridge (3-wire or 4-wire)			
Ranges	2 mV/V...1000 mV/V free programmable with Dual Core			
Internal Bridge Completion	Half and Quarter bridge 120 Ω and 350 Ω			
Typ. Bridge Completion Accuracy	0.05 %; TCR: 2 ppm/K (others on request)			
Internal Shunt Resistor	59.88 kΩ, 175 kΩ, software selectable (others on request)			
Typ. Shunt Resistor Accuracy	0.05 %; TCR: 10 ppm/K (others on request)			
Input Short, Sensor Offset Adjust	Software selectable			
Counters (only on STG+ type)				
Inputs	1 digital counter input 3 digital inputs Fully synchronised with analog data Alarm output			
Counter Modes	counting, waveform timing, encoder, tacho, gear-tooth sensor			
General Counter Specifications	See "SIRIUS counter specifications"			
Additional Specifications				
Input connector	DSUB-9, 8-pin LEMO-2B, 16-pin LEMO-2B (others on request)			
TEDS support	Standard + DSI® adapters			

Appendix 2. Part of the Modbus channel list displayed in DewesoftX.

+	ID	Used	C	Name
				--- Plugins ---
	2	Used		A_in 1 Diesel pressure DE
	3	Used		A_in 3 HT pressure jacket in
	4	Used		A_in 4 LT water pressure CAC in
	5	Used		A_in 5 LO pressure TC in
	6	Used		A_in 7 FO-pressure engine inlet
	7	Used		A_in 8 CA-pressure engine inlet
	8	Used		A_in 9 Start air pressure engine in
	9	Used		A_in 10 Lub oil pressure engine in
	10	Used		A_in 11 Lub oil pressure filter in
	11	Used		A_in 12 Crank case pressure
	12	Used		A_in 14 Engine load feedback
	13	Used		Pr. b Turbine (p5) lower
	14	Used		Pr. CA b CAC (p2)
	15	Used		A1_out 1 LT cooling water therm...
	16	Used		A1_out 3 Engine speed
	17	Used		Analogue speed reference
	18	Used		Engine load kW
	19	Used		Engine load mbar
	20	Used		Engine load pph
	21	Used		Measured engine speed
	22	Used		Engine speed reference
	23	Used		External load reference
	24	Used		Load reference kW
	25	Used		Fuel demand pptt
	26	Used		Diesel demand compensated
	27	Used		Diesel demand
	28	Used		FCV position ppt
	29	Used		CA-pressure deviation from refe...
	30	Used		CA-temp deviation from reference
	31	Used		AWG position
	32	Used		Miller timing on/off
	33	Used		TC speed
	34	Used		MFI offsets diesel cyl1

Appendix 3. Example text-file export from DewesoftX.

Data1

X axis	IV position_ds_4	EV position_ds_4	IV control_ds_4	EV control_ds_4
-	mm	mm	%	%
-360.00	10.18	7.81	61.35	36.59
-359.90	10.23	7.75	61.07	36.16
-359.80	10.28	7.73	59.86	35.29
-359.70	10.31	7.67	59.82	35.29
-359.60	10.33	7.60	59.81	35.28
-359.50	10.38	7.57	59.83	35.25
-359.40	10.39	7.56	59.99	35.40
-359.30	10.44	7.51	61.23	36.54
-359.20	10.50	7.49	61.35	36.58
-359.10	10.54	7.47	61.34	36.59
-359.00	10.58	7.43	61.44	36.61
-358.90	10.59	7.43	61.38	36.25
-358.80	10.64	7.38	59.74	28.31
-358.70	10.68	7.32	59.84	30.33
-358.60	10.70	7.26	59.81	30.30
-358.50	10.74	7.23	59.80	30.23
-358.40	10.80	7.21	59.80	31.36
-358.30	10.80	7.20	59.80	31.42
-358.20	10.84	7.15	59.81	31.54
-358.10	10.89	7.13	59.81	31.58
-358.00	10.93	7.09	59.80	31.65
-357.90	10.95	7.03	59.80	30.55
-357.80	10.95	7.03	59.80	30.40
-357.70	11.01	6.99	59.79	30.28
-357.60	11.02	6.93	59.77	30.24
-357.50	11.06	6.88	59.78	30.19
-357.40	11.11	6.87	58.53	31.16
-357.30	11.17	6.85	58.27	31.55
-357.20	11.17	6.84	58.27	31.55
-357.10	11.21	6.80	58.23	31.53
-357.00	11.24	6.76	58.24	31.40
-356.90	11.25	6.69	58.22	30.48
-356.80	11.27	6.63	58.22	30.21
-356.70	11.28	6.62	58.22	30.22
-356.60	11.32	6.59	58.21	30.20
-356.50	11.35	6.55	58.16	30.22
-356.40	11.39	6.52	59.05	31.04
-356.30	11.44	6.50	59.78	31.53
-356.20	11.45	6.50	59.82	31.54
-356.10	11.48	6.44	59.77	31.53
-356.00	11.51	6.41	59.84	31.55
-355.90	11.52	6.35	58.34	30.86
-355.80	11.54	6.30	56.71	30.21
-355.70	11.58	6.27	56.76	30.25
-355.60	11.59	6.27	56.76	30.25
-355.50	11.62	6.21	56.89	30.20
-355.40	11.65	6.18	57.81	30.76
-355.30	11.67	6.13	58.25	31.54

Appendix 4. Analog signal error calculations in the high sampling frequency measurement chain.

Parameter	Description	Instrument error (%)	Conversion error (%)	ADC gain error (%)	Error (%) = $\pm\sqrt{Instrument\ error^2 + Conversion\ error^2 + ADC\ gain\ error^2}$
Cyl1_p	In-cylinder pressure	0.5	1	0.05	±1.119
Cyl2_p	In-cylinder pressure	0.5	1	0.05	±1.119
Cyl3_p	In-cylinder pressure	0.5	1	0.05	±1.119
Cyl4_p	In-cylinder pressure	0.5	1	0.05	±1.119
Intake_p	Intake port pressure	1.0	0.5	0.05	±1.119
Exhaust_p	Exhaust port pressure	0.3	0.5	0.05	±0.585
FastNOx_ppm	Fast NOx measurement	1.0	0	0.05	±1.001
FastTHC_ppm	Fast THC measurement	1.0	0	0.05	±1.001
IV_position	Intake valve position	0.2	1	0.05	±1.021
EV_position	Exhaust valve position	0.2	1	0.05	±1.021
IV_control	Intake valve cntrol signal	0	0	0.05	±0.05
EV_control	Exhaust valve cntrol signal	0	0	0.05	±0.05

Appendix 5. Measured analog signal curves during the EHVA unit test representing the valve position and control signals in time domain.